The FFTRR based Fast Direct Algorithms for Complex Inhomogeneous Biharmonic Problems with Applications to Incompressible Flows

Prabir Daripa* and Aditi Ghosh†

Department of Mathematics, Texas A&M University, College Station, TX-77843

October 18, 2016

Abstract

We develop analysis based fast and accurate **direct** algorithms for several biharmonic problems in a unit disk derived directly from the Green's functions of these problems, and compare the numerical results with the "decomposition" algorithms (see [17]) in which the biharmonic problems are first decomposed into lower order problems, most often either into two Poisson problems or into two Poisson problems and a homogeneous biharmonic problem. One of the steps in the "decomposition algorithm" as discussed in [17] for solving certain biharmonic problems uses the "direct algorithm" without which the problem can not be solved. Using classical Green's function approach for these biharmonic problems, solutions of these problems are represented in terms of singular integrals in the complex $z-$plane (the physical plane) involving explicitly the boundary conditions. Analysis of these singular integrals using FFT and recursive relations (RR) in Fourier space leads to the development of these fast algorithms which are called **FFTRR** based algorithms. These algorithms do not need to do anything special to overcome co-ordinate singularity at the origin as often the case when solving these problems using finite difference methods in polar coordinates. These algorithms have some other desirable properties such as the ease of implementation and parallel in nature by construction. Moreover, these algorithms have $O(\log N)$ complexity per grid point where N^2 is the total number of grid points and have very low constant behind this order estimate of the complexity. Performance of these algorithms is shown on several test problems. These algorithms are applied to solving viscous flow problems at low and moderate Reynolds numbers and numerical results are presented.

1 Introduction

In this paper, we consider boundary value problems for the inhomogeneous complex biharmonic equation

$$(\partial_z \partial_{\bar{z}})^2 \omega = f(z, \bar{z}), \tag{1}$$

in the complex z-plane which is the physical $x - y$ plane through the assignment $z = x + iy$. Note that the left hand operator of the above equation is the biharmonic operator Δ^2 in the physical (real) plane except for a factor of $1/16$ (i.e., $(\partial_z \partial_{\bar{z}})^2 = \Delta^2/16$), thus the above equation corresponds to two uncoupled biharmonic equations in the physical plane provided the inhomogeneous term f does not depend on the solution ω and it can be separated into real and imaginary parts. However, problems associated with these two uncoupled biharmonic equations can be coupled through the boundary conditions in which case these two coupled problems can be solved simultaneously by solving the boundary value problem (see the problem (D1) in section 2 below) for the complex biharmonic equation (1). When the source term f is real and the prescribed boundary values

---

2

are real, we recover the conventional inhomogeneous biharmonic problem in the physical plane. Thus, the complex biharmonic equation is a more general case and can be used to solve biharmonic problems in the physical plane as well as in the complex plane.

It should be mentioned that numerical solutions of biharmonic problems in real plane are constructed by a variety of methods including finite difference [7, 31] (see also references therein), finite element [8, 11, 12, 29, 32], and integral equation methods [18, 19, 20, 27]. Importance of solving biharmonic problems in the physical plane can not be over-emphasized as they also arise as an intermediary step in solving many linear and nonlinear elliptic and parabolic problems such as problems involving the Navier-Stokes equations and so on; see [21, 24, 30]. The complex biharmonic problems, even though less common in applications, do arise (see [30, 35]). Because they do not arise that often, these have not received much attention except in the most recent work of the authors [17] on the decomposition approach. This paper is a sequel to [17].

There are following two general approaches for solving inhomogeneous biharmonic problems: (i) the decomposition method in which inhomogeneous biharmonic problems are decomposed into two Poisson problems and **also one homogeneous biharmonic problem** in some cases, as further discussed in the following paragraph. The homogeneous biharmonic problems are solved in [17] by the direct approach which we discuss in this paper for the first time. The fast algorithms based on the first approach (i.e., the decomposition method) has been recently addressed in [17]; and (ii) the **direct** method in which these problems are solved **directly** without the use of lower order problems such as Poisson problems. This paper is about fast algorithms based on this direct method in which the classical Green's function approach provides integral representations for the solutions of the biharmonic problems in the **complex z-plane** (physical plane). Existence of solutions and their integral representations for four types of biharmonic problems in a unit disk have been recently provided by Begehr [3, 4, 5, 6]. The boundary and domain integrals involved in these representations are singular. It is well established (see [2, 10, 13, 14, 15, 17]) by now that the use of FFT and Recursive Relations (RR) for the evaluation of these singular integrals results in fast and accurate algorithms. However, it requires analysis in the complex plane and careful synthesis of various components to develop the RR relations as we will see in this paper.

There are several reasons for the development of fast algorithms based on this direct method. Firstly, solving homogeneous biharmonic problems using the direct method presented in this paper requires evaluation of boundary integrals only which can be done rapidly with spectral accuracy as we will see in section 5. On the other hand, solving these homogeneous problems using the decomposition method of [17] significantly reduces the order of accuracy (depending on the quadrature method used) and increase computational time because the method requires evaluation of volume integrals since one of the two decomposed problems in this method is a Poisson problem (see [17]). Moreover, as we have seen in Ghosh and Daripa [17], solving two of the four boundary value problems ((D1) and (D3) problems) by the decomposition method requires solving homogeneous biharmonic problems which are efficiently done by the method proposed here. Secondly, the algorithms based on the direct method is worth comparing to those ([17]) based on the decomposition method. The pros and cons of these two different approaches have been discussed later when we discuss numerical results.

In the FFTRR based method, we expand the integrals in terms of their Fourier series and derive their radius dependent Fourier coefficients in terms of one dimensional non-singular integrals. These one-dimensional integrals bear some recursive relations which are at the heart of the low computational cost of the full algorithms for solving these inhomogeneous biharmonic problems. There are several such singular integrals which appear in the integral representation of solutions of these problems. FFTRR based method is applied to each one of these and the resulting formulas are integrated together in an efficient way that give rise to the fast and accurate algorithms for solving these biharmonic problems. These algorithms do not need to do anything special to overcome the co-ordinate singularity at the origin as often the case when solving these problems in polar coordinates using finite difference methods.

In this paper, we develop such FFTRR based fast algorithms for four different types of biharmonic problems inside a unit disk. The problems chosen serve only as examples for many other complex biharmonic problems (see Begehr [3, 4, 5, 6]) for which similar FFTRR based fast algorithms can be developed, if desired, using the procedure outlined here. The FFTRR formulas which make up the algorithms given in the section 3 do not need to be translated in real variables

for application of the fast algorithms to solving real biharmonic problems. However, a complex rewriting of the real biharmonic problem is necessary for application of the fast algorithms. This is exemplified in section 5 where we solve steady incompressible Navier-Stokes equations in the physical plane. Many problems in plane elasticity [30, 35] are also naturally formulated as complex biharmonic problems whose solutions can be computed using the fast algorithms developed in this paper. It is conjectured that complex biharmonic problems can play an important role in applied mathematics and classical physics.

The algorithms developed in this paper enjoy many desired properties which include the following: (i) low asymptotic computational complexity: $\mathcal{O}(\log N)$ per point where N^2 is the total number of grid points; (ii) very low value of the constant in this order estimate meaning the ratio of computational time to $(N^2 \log N)$ is small and weakly dependent of N for large N; (iii) parallel by construction; (iv) easy to implement; (v) high order accurate (with further qualification, see section 4) without additional grid points for the integration of one-dimensional integrals that appear in these algorithms; and (vi) easily adapted to non-uniform grids as well as to weakly singular source terms in the inhomogeneous biharmonic equations. All of the properties will be evident from expositions in this paper except that the last property, namely (vi), falls outside the scope of this paper and property (iii), which should be transparent, nonetheless has been briefly explained in section 3.4. based on a desired accuracy: this has been addressed in [17] where we solve the biharmonic problems by using the decomposition method.

This paper is laid out as follows. In section 2, we present four different types of biharmonic problems, the integral representations of their solutions arising from Green's function approach, and the analysis of these representations using FFTRR method leading to the development of the basic ingredients for the fast algorithms presented in section 3. Numerical results are presented in section 4. These algorithms are applied to solving low to moderate Reynolds number fluid flow problems in section 5. Finally we conclude in section 6. In the appendix, we give the proofs of various theorems presented in section 2.

2   Biharmonic problems

In this section, we use the **direct** approach and develop the mathematical foundation of fast algorithms for four different types of biharmonic problems ((D1), (D2), (D3) and (D4), see below) in a unit disc $\mathbf{D} = \{z \in \mathbb{C}, |z| \leq 1\}$ in the complex plane. Each problem is distinguished by a different boundary condition. Using the classical Green's function approach, integral representations of the solutions of these problems have been recently provided by Begehr [5]. These integral representations involve weakly singular integrals (see the area integrals in Theorems 1, 3, 5, and 7 below in this section) whose analysis for the purpose of fast and accurate evaluation is performed in this section. The theorems resulting from this analysis to be used in the development of the fast algorithms given in the section 3 are given below and their proofs are given in the appendix. We should mention here that the existence of solutions to problems (D2) and (D4) defined below is given under the assumption that the inhomogeneous term $f \in L_p(\mathbf{D}; \mathbb{C}), p > 2$ (see Begehr [5]). However, we develop the algorithms for constructing solutions of these problems numerically under the assumption that is expandable in a Fourier series.

2.1   Dirichlet problem of type (D1)

We first consider the biharmonic equation with Dirichlet-1 (or (D1)) type boundary conditions. This problem arises in plane elasticity [30].

$$\left. \begin{array}{rll} (\partial_z \partial_{\bar{z}})^2 \omega &= f, & \text{in} \ \ \mathbf{D}, \\ \omega &= h_0, & \text{on} \ \ \partial \mathbf{D}, \\ \partial_{\bar{z}} \omega &= h_1, & \text{on} \ \ \partial \mathbf{D}. \end{array} \right\} \tag{D1}$$

Henceforth we refer to it as the (D1) problem. In this and all problems described below, the inhomogeneous term f and the boundary data (such as h_0 and h_1 for the above problem) associated with each problem will in general be functions of one or both the variables: z and $\bar{z}$. It is worth mentioning here that this problem can not be decomposed into two Poisson problems only. In

order to develop the fast algorithm in this **direct** approach, we use the following theorem from Begehr [5].

Theorem 1. *The Dirichlet-1* (D1) *biharmonic problem is uniquely solvable for $f \in L_2(\mathbf{D}; \mathbb{C})$, $h_0 \in C^2(\partial\mathbf{D}, \mathbb{C})$, $h_1 \in C(\partial\mathbf{D}, \mathbb{C})$. Its solution is given by*

$$\omega(z) = u_2(z) + v_2(z) + r_2(z) + \hat{G}f(z) \tag{2}$$

where

$$u_2(z) = \frac{1}{2\pi i} \int_{\partial\mathbf{D}} g_1(z, \zeta) h_0(\zeta) \frac{d\zeta}{\zeta}, \tag{3}$$

$$v_2(z) = \frac{(1 - |z|^2)}{2\pi i} \int_{\partial\mathbf{D}} \frac{z\bar{\zeta}}{(1 - z\bar{\zeta})^2} h_0(\zeta) \frac{d\zeta}{\zeta}, \tag{4}$$

$$r_2(z) = -\frac{(1 - |z|^2)}{2\pi i} \int_{\partial\mathbf{D}} g_1(z, \zeta) h_1(\zeta) d\bar{\zeta}, \tag{5}$$

$$\hat{G}f(z) = -\frac{1}{\pi} \iint_{\mathbf{D}} G_2(z, \zeta) f(\zeta) d\xi d\eta, \quad \zeta = \xi + i\,\eta, \tag{6}$$

$$G_2(z, \zeta) = |\zeta - z|^2 \log \left| \frac{1 - z\bar{\zeta}}{\zeta - z} \right|^2 - (1 - |z|^2)(1 - |\zeta|^2), \tag{7}$$

$$g_1(z, \zeta) = -\frac{1}{2}\partial_\nu G_1(z, \zeta) = \frac{1}{1 - z\bar{\zeta}} + \frac{1}{1 - \bar{z}\zeta} - 1. \tag{8}$$

Here $G_2(z, \zeta)$ is the Green's function for the (D1) *biharmonic problem but with homogeneous boundary conditions and G_1 is the harmonic Green's function.*

We write $\hat{G}f(z)) = I_3(z) + I_4(z) + I_5(z)$, where

$$I_3(z) = \frac{(1 - |z|^2)}{\pi} \iint_{\mathbf{D}} f(\zeta)(1 - |\zeta|^2) d\xi d\eta, \tag{9}$$

$$I_4(z) = -\frac{2}{\pi} \iint_{\mathbf{D}} |\zeta - z|^2 \log|1 - z\bar{\zeta}| f(\zeta) d\xi d\eta, \tag{10}$$

$$I_5(z) = \frac{2}{\pi} \iint_{\mathbf{D}} |\zeta - z|^2 \log|\zeta - z| f(\zeta) d\xi d\eta. \tag{11}$$

The Fourier coefficients of the solution $\omega(z)$ to the (D1) biharmonic problem is embedded in the following theorem. Its proof is given in the Appendix.

Theorem 2. *If $\omega(r, \alpha)$ is the solution of the* (D1) *biharmonic problem, $z = re^{i\alpha}$, $f(re^{i\alpha}) = \sum_{n=-\infty}^{\infty} f_n(r)e^{in\alpha}$, $h_0(e^{i\alpha}) = \sum_{n=-\infty}^{\infty} a_n e^{in\alpha}$, and $h_1(e^{i\alpha}) = \sum_{n=-\infty}^{\infty} b_n e^{in\alpha}$, then the Fourier coefficients $\omega_n(r)$ of $\omega(z)$ can be written as*

$$\omega_n(r) = I_{3,n}(r) + I_{4,n}(r) + I_{5,n}(r) + u_{2,n}(r) + v_{2,n}(r) + r_{2,n}(r),$$

where

$$u_{2,n}(r) = \begin{cases} a_n r^{|n|}, & if \quad n \neq 0, \\ a_0, & if \quad n = 0, \end{cases} \tag{12}$$

$$v_{2,n}(r) = \begin{cases} (1 - r^2)\frac{(2)_{n-1}}{(n-1)!} r^n a_n, & if \quad n \geq 1, \\ 0, & if \quad n < 1, \end{cases} \tag{13}$$

where $(x)_n = \frac{\Gamma(x+n)}{\Gamma(x)}$,

$$r_{2,n}(r) = \begin{cases} b_{1+n} r^{|n|}(1-r^2), & \text{if } n \neq 0, \\ b_1(1-r^2), & \text{if } n = 0, \end{cases} \tag{14}$$

$$I_{3,n}(r) = \begin{cases} 2(1-r^2)\int_0^1 f_0(\rho)\,\rho(1-\rho^2)\,d\rho, & \text{if } n = 0, \\ 0, & \text{if } n \neq 0. \end{cases} \tag{15}$$

Moreover, $I_{4,n} = I_{4,n}^{(1)} + I_{4,n}^{(2)} + I_{4,n}^{(3)} + I_{4,n}^{(4)}$ where

$$I_{4,n}^{(1)}(r) = \begin{cases} 2r^2 \int_0^1 f_n(\rho)\frac{(r\rho)^{|n|}}{|n|}\rho\,d\rho, & \text{if } n \neq 0, \\ 0, & \text{if } n = 0, \end{cases} \tag{16}$$

$$I_{4,n}^{(2)}(r) = \begin{cases} 2 \int_0^1 f_n(\rho)\frac{(r\rho)^{|n|}}{|n|}\rho^3\,d\rho, & \text{if } n \neq 0, \\ 0, & \text{if } n = 0, \end{cases} \tag{17}$$

$$I_{4,n}^{(3)}(r) = \begin{cases} -\frac{2}{(n+1)}\int_0^1 f_n(\rho)(r\rho)^{n+2}\rho\,d\rho, & \text{if } n > -1, \\ \frac{2}{(n+1)}\int_0^1 f_n(\rho)(r\rho)^{-n}\rho\,d\rho, & \text{if } n < -1, \\ 0, & \text{if } n = -1, \end{cases} \tag{18}$$

$$I_{4,n}^{(4)}(r) = \begin{cases} -\frac{2}{(n-1)}\int_0^1 f_n(\rho)(r\rho)^{n}\rho\,d\rho, & \text{if } n > 1, \\ \frac{2}{(n-1)}\int_0^1 f_n(\rho)(r\rho)^{2-n}\rho\,d\rho, & \text{if } n < 1, \\ 0, & \text{if } n = 1. \end{cases} \tag{19}$$

and $I_{5,n} = I_{5,n}^{(1)} + I_{5,n}^{(2)} + I_{5,n}^{(3)} + I_{5,n}^{(4)}$ where

$$I_{5,n}^{(1)}(r) = \begin{cases} -2r^2\left[\int_0^r f_n(\rho)(\frac{\rho}{r})^{|n|}\frac{\rho}{|n|}d\rho + \int_r^1 f_n(\rho)(\frac{r}{\rho})^{|n|}\frac{\rho}{|n|}d\rho\right], & \text{if } n \neq 0, \\ 4r^2\left[\int_0^r f_0(\rho)\left(\frac{\rho}{r}\right) r\log r\,d\rho + \int_r^1 f_0(\rho)\rho\log\rho\,d\rho\right], & \text{if } n = 0, \end{cases} \tag{20}$$

$$I_{5,n}^{(2)}(r) = \begin{cases} \frac{-2}{|n|}\left[\int_0^r f_n(\rho)(\frac{\rho}{r})^{|n|}\rho^3 d\rho + \int_r^1 f_n(\rho)(\frac{r}{\rho})^{|n|}\rho^3 d\rho\right], & \text{if } n \neq 0, \\ 4\left[\int_0^r f_0(\rho)\left(\frac{\rho}{r}\right)^3 r^3\log r\,d\rho + \int_r^1 f_0(\rho)\rho^3\log\rho\,d\rho\right], & \text{if } n = 0, \end{cases} \tag{21}$$

$$I_{5,n}^{(3)}(r) = \begin{cases} \frac{2r}{|n+1|}\left[\int_0^r f_n(\rho)(\frac{\rho}{r})^{|n+1|}\rho^2 d\rho + \int_r^1 f_n(\rho)(\frac{r}{\rho})^{|n+1|}\rho^2 d\rho\right], & \text{if } n \neq -1, \\ -4r\left[\int_0^r f_{-1}(\rho)\rho^2\log r\,d\rho + \int_r^1 f_{-1}(\rho)\rho^2\log\rho\,d\rho\right], & \text{if } n = -1, \end{cases} \tag{22}$$

$$I_{5,n}^{(4)}(r) = \begin{cases} \frac{2r}{|n-1|}\left[\int_0^r f_n(\rho)(\frac{\rho}{r})^{|n-1|}\rho^2 d\rho + \int_r^1 f_n(\rho)(\frac{r}{\rho})^{|n-1|}\rho^2 d\rho\right], & \text{if } n \neq 1, \\ -4r\left[\int_0^r f_1(\rho)\rho^2\log r\,d\rho + \int_r^1 f_1(\rho)\rho^2\log\rho\,d\rho\right], & \text{if } n = 1. \end{cases} \tag{23}$$

2.2 Dirichlet problem of type (D2)

Consider the biharmonic equation with Dirichlet-2 (or (D2)) type boundary conditions. The following theorem is taken from Begehr [5]. This problem is sometimes called Riquier and also Navier problem. This problem arises in the theory of elasticity, specially in modeling bending of plates (see [25]).

Theorem 3. *The Dirichlet-2 problem for the biharmonic equation given by*

$$\left.\begin{array}{rlll}
(\partial_z \partial_{\bar{z}})^2 \omega & = f, & in & \mathbf{D}, \\
\omega & = h_0, & on & \partial\mathbf{D}, \\
\partial_z \partial_{\bar{z}} \omega & = h_2, & on & \partial\mathbf{D}.
\end{array}\right\} \tag{D2}$$

is uniquely solvable for $f \in L_p(\mathbf{D}; \mathbb{C}), p > 2$, $h_0 \in C(\partial\mathbf{D}; \mathbb{C})$, $h_2 \in C(\partial\mathbf{D}; \mathbb{C})$ and the solution is given by

$$\omega(z) \;\; = \;\; u_2(z) + v_3(z) + Gf(z),$$

where

$$u_2(z) \;\; = \;\; \frac{1}{2\pi i} \int_{\partial\mathbf{D}} g_1(z, \zeta) h_0(\zeta) \frac{d\zeta}{\zeta}, \tag{24}$$

$$v_3(z) \;\; = \;\; \frac{1}{2\pi i} \int_{\partial\mathbf{D}} H_2(z, \zeta) h_2(\zeta) \frac{d\zeta}{\zeta}, \tag{25}$$

$$Gf(z) \;\; = \;\; -\frac{1}{\pi} \iint_{\mathbf{D}} G_{12}(z, \zeta) f(\zeta) d\xi d\eta, \tag{26}$$

$$H_2(z, \zeta) \;\; = \;\; (1 - |z|^2) \left[\frac{1}{z\bar{\zeta}} \log(1 - z\bar{\zeta}) + \frac{1}{\bar{z}\zeta} \log(1 - \bar{z}\zeta) + 1 \right], \tag{27}$$

$$G_{12}(z, \zeta) \;\; = \;\; |\zeta - z|^2 \log \left| \frac{1 - z\bar{\zeta}}{\zeta - z} \right|^2 + (1 - |z|^2)(1 - |\zeta|^2) \left[\frac{\log(1 - z\bar{\zeta})}{z\bar{\zeta}} + \frac{\log(1 - \bar{z}\zeta)}{\bar{z}\zeta} \right]. \tag{28}$$

Here $G_{12}(z, \zeta)$ is the Green's function for the (D2) *biharmonic problem but with homogeneous boundary conditions and $g_1(z, \zeta)$ in (24) is given by (8).*

Substituting the expressions for $H_2(z, \zeta)$ from (27) in (25), we obtain the following integral representation for $v_3(z)$.

$$v_3(z) = \frac{1}{2\pi i}(1 - |z|^2) \int_{\partial\mathbf{D}} \frac{h_2(\zeta) \log(1 - z\bar{\zeta})}{z|\zeta|^2} d\zeta + \frac{1}{2\pi i}(1 - |z|^2) \int_{\partial\mathbf{D}} \frac{h_2(\zeta) \log(1 - \zeta\bar{z})}{\bar{z}\zeta^2} d\zeta$$

$$+ \frac{1}{2\pi i}(1 - |z|^2) \int_{\partial\mathbf{D}} h_2(\zeta) \frac{d\zeta}{\zeta}.$$

$$= v_3^{(1)}(z) + v_3^{(2)}(z) + v_3^{(3)}(z). \tag{29}$$

Also substituting $G_{12}(z, \zeta)$ from (28) in (26) and recalling $\zeta = \xi + i\eta$, we obtain

$$Gf(z) = I_4(z) + I_5(z) + I_6(z) + I_7(z), \tag{30}$$

where $I_4(z)$ and $I_5(z)$ are given before (see (10) and (11)) and

$$I_6(z) \;\; = \;\; -\frac{1}{\pi} \frac{(1 - |z|^2)}{z} \iint_{\mathbf{D}} (1 - |\zeta|^2) \frac{\log(1 - \bar{\zeta}z)}{\bar{\zeta}} f(\zeta) d\xi d\eta, \tag{31}$$

$$I_7(z) \;\; = \;\; -\frac{1}{\pi} \frac{(1 - |z|^2)}{\bar{z}} \iint_{\mathbf{D}} (1 - |\zeta|^2) \frac{\log(1 - \bar{z}\zeta)}{\zeta} f(\zeta) d\xi d\eta. \tag{32}$$

We develop fast and accurate algorithms to evaluate the singular integrals appearing above in the expression of $Gf(z)$. Since we assume f is smooth, the integrands in these integrals have removable singularities. As we will see below, evaluation of the Fourier coefficients of these integrals using the following theorem (for proof, see the Appendix) leads to evaluation of one-dimensional nonsingular integrals in the fast algorithm for solving the (D2) biharmonic problem.

Theorem 4. *If $\omega(r, \alpha)$ is the solution of the (D2) biharmonic problem, $z = re^{i\alpha}$, $f(re^{i\alpha}) = \sum_{n=-\infty}^{\infty} f_n(r)e^{in\alpha}$, $h_0(e^{i\alpha}) = \sum_{n=-\infty}^{\infty} a_n e^{in\alpha}$, and $h_2(e^{i\alpha}) = \sum_{n=-\infty}^{\infty} c_n e^{in\alpha}$, then the Fourier coefficients $\omega_n(r)$ of $\omega(r, \alpha)$ can be written as*

$$\omega_n(r) = I_{4,n}(r) + I_{5,n}(r) + I_{6,n}(r) + I_{7,n}(r) + u_{2,n}(r) + v_{3,n}(r),$$

where $I_{4,n}(r), I_{5,n}(r)$ and $u_{2,n}(r)$ are same as in Thm. 2 and

$$I_{6,n}(r) = \begin{cases} \frac{2(1-r^2)r^n}{(n+1)} \int_0^1 f_n(\rho)\, \rho^{(n+1)}(1-\rho^2)\, d\rho, & \text{if } n \geq 0, \\ 0, & \text{if } n < 0, \end{cases} \tag{33}$$

$$I_{7,n}(r) = \begin{cases} \frac{2(1-r^2)r^{-n}}{(1-n)} \int_0^1 f_n(\rho)\, \rho^{(1-n)}(1-\rho^2)\, d\rho, & \text{if } n \leq 0, \\ 0. & \text{if } n > 0, \end{cases} \tag{34}$$

$$v_{3,n}(r) = \begin{cases} \frac{c_n(r^{|n|+2}-r^{|n|})}{n+1}, & \text{if } n \neq 0, \\ c_0(1-r^2), & \text{if } n = 0. \end{cases} \tag{35}$$

Next we consider two biharmonic problems having Neumann type boundary conditions.

2.3 Dirichlet-Neumann problem of type (D3)

The first problem we consider with Neumann type boundary conditions is called the Dirichlet-Neumann1(D3) biharmonic problem below. This problem arises in radar imaging [1] as well as in fluid mechanics. The following theorem is taken from Begehr [5].

Theorem 5. *The Dirichlet-Neumann1(D3) biharmonic problem is given by*

$$\left. \begin{aligned} (\partial_z \partial_{\bar{z}})^2 \omega &= f, & in \quad \mathbf{D}, \\ \omega &= h_0, & on \quad \partial\mathbf{D}, \\ \partial_\nu \omega &= h_1, & on \quad \partial\mathbf{D}, \end{aligned} \right\} \tag{D3}$$

is uniquely solvable for $f \in L_1(\mathbf{D}; \mathbb{C})$, $h_0 \in C^2(\partial\mathbf{D}; \mathbb{C})$, and $h_1 \in C^1(\partial\mathbf{D}; \mathbb{C})$. The integral representation of its solution based on classical Green's function approach [5] is given by

$$\omega(z) = \frac{(1+|z|^2)}{4\pi i} \int_{\partial\mathbf{D}} g_1(z, \zeta) h_0(\zeta) \frac{d\zeta}{\zeta} + \frac{(1-|z|^2)}{4\pi i} \int_{\partial\mathbf{D}} g_2(z, \zeta) h_0(\zeta) \frac{d\zeta}{\zeta}$$

$$- \frac{(1-|z|^2)}{2\pi i} \int_{\partial\mathbf{D}} g_1(z, \zeta) h_1(\zeta) \frac{d\zeta}{\zeta} - \frac{1}{\pi} \iint_{\mathbf{D}} G_2(z, \zeta) f(\zeta) d\xi d\eta,$$

where

$$g_2(z, \zeta) = \frac{1}{(1-z\bar{\zeta})^2} + \frac{1}{(1-\bar{z}\zeta)^2} - 1,$$

and $G_2(z, \zeta)$, $g_1(z, \zeta)$ are given by (3) and (8) respectively. We again remind here that $\zeta = \xi + i\eta$.

We write $\omega(z)$ as

$$\omega(z) = u_3(z) + h_3(z) + r_3(z) + I_3(z) + I_4(z) + I_5(z) \tag{36}$$

where

$$u_3(z) = \frac{(1+|z|^2)}{4\pi i} \int_{\partial\mathbf{D}} g_1(z, \zeta) h_0(\zeta) \frac{d\zeta}{\zeta}, \tag{37}$$

$$h_3(z) = \frac{(1-|z|^2)}{4\pi i} \int_{\partial\mathbf{D}} g_2(z, \zeta) h_0(\zeta) \frac{d\zeta}{\zeta}, \tag{38}$$

$$r_3(z) = -\frac{(1-|z|^2)}{4\pi i} \int_{\partial\mathbf{D}} g_1(z, \zeta) h_1(\zeta) \frac{d\zeta}{\zeta}. \tag{39}$$

The terms $I_3(z), I_4(z)$ and $I_5(z)$ are given in (9), (10), and (11) respectively. Evaluation of the Fourier coefficients of these integrals using the following theorem (for a proof, see the Appendix) will lead to the desired fast algorithm for solving the (D3) biharmonic problem.

Theorem 6. *If $\omega(r, \alpha)$ is the solution of the (D3) biharmonic problem defined in Thm. 5, $z = re^{i\alpha}$,*
$$f(re^{i\alpha}) = \sum_{n=-\infty}^{\infty} f_n(r)e^{in\alpha}, \quad h_0(e^{i\alpha}) = \sum_{n=-\infty}^{\infty} a_n e^{in\alpha}, \quad and \quad h_1(e^{i\alpha}) = \sum_{n=-\infty}^{\infty} b_n e^{in\alpha}, \quad then \; the \; Fourier$$
coefficients $\omega_n(r)$ of $\omega(r, \alpha)$ can be written as

$$\omega_n(r) = I_{3,n}(r) + I_{4,n}(r) + I_{5,n}(r) + u_{3,n}(r) + h_{3,n}(r) + r_{3,n}(r),$$

where the Fourier coefficients of the boundary integrals are given by

$$u_{3,n}(r) = \begin{cases} \frac{1+r^2}{2} r^{|n|} a_n, & if \; n \neq 0, \\ \frac{1+r^2}{2} a_0, & if \; n = 0, \end{cases}$$

$$h_{3,n}(r) = \begin{cases} \frac{(1-r^2)}{2} \frac{(2)_{|n|}}{|n|} r^{|n|} a_n, & if \; n \neq 0, \\ \frac{(1-r^2)}{2} a_0, & if \; n = 0, \end{cases}$$

$$r_{3,n}(r) = \begin{cases} -\frac{(1-r^2)}{2} b_n r^{|n|}, & if \; n \neq 0, \\ -\frac{(1-r^2)}{2} b_0, & if \; n = 0. \end{cases}$$

The Fourier coefficients $I_{3,n}(r), I_{4,n}(r)$ and $I_{5,n}(r)$ have already been evaluated in Thm. 2.

2.4 Dirichlet-Neumann problem of type (D4)

We now consider a second kind of biharmonic problems called Dirichlet-Neumann2 (D4) biharmonic problem. The following theorem is taken from Begehr [5].

Theorem 7. *The Dirichlet-Neumann2 (D4) biharmonic problem given by*

$$\left. \begin{array}{rlll} (\partial_z \partial_{\bar{z}})^2 w &= f, & in & \mathbf{D}, \\ w &= h_0, & on & \partial\mathbf{D}, \\ \partial_\nu w_{z\bar{z}} &= h_2, & on & \partial\mathbf{D}, \\ k &= \frac{1}{2\pi i} \int_{\partial\mathbf{D}} w_{z\bar{z}}(z) \frac{dz}{z} \end{array} \right\} \tag{D4}$$

is uniquely solvable for $f \in L_p(\mathbf{D}; \mathbb{C}), p > 2, h_0, \; h_2 \in (\partial\mathbf{D}; \mathbb{C})$ if and only if $\frac{1}{4i} \int_{\partial\mathbf{D}} h_2(\zeta)\frac{d\zeta}{\zeta} = \int_{\mathbf{D}} f(\zeta)d\xi d\eta$ and the solution obtained directly using the Green's function is given by

$$w(z) = k(|z|^2 - 1) + \frac{1}{2\pi i} \int_{\partial\mathbf{D}} g_1(z, \zeta)h_0(\zeta)\frac{d\zeta}{\zeta} + \frac{1}{4\pi i} \int_{\partial\mathbf{D}} G_{13}(z, \zeta)h_2(\zeta)\frac{d\zeta}{\zeta}$$

$$- \frac{1}{\pi} \iint_{\mathbf{D}} G_{13}(z, \zeta)f(\zeta)d\xi d\eta, \tag{40}$$

where $g_1(z, \zeta)$ is the function defined in (8), and

$$G_{13}(z, \zeta) = -|\zeta - z|^2 \log|\zeta - z|^2$$

$$- (1 - |z|^2)\left(4 + \frac{(1 - z\bar{\zeta})}{z\bar{\zeta}} \log(1 - z\bar{\zeta}) + \frac{(1 - \bar{z}\zeta)}{\bar{z}\zeta} \log(1 - \bar{z}\zeta) \right)$$

$$- \frac{(\zeta - z)(1 - z\bar{\zeta})}{z} \log(1 - z\bar{\zeta}) - \frac{\overline{(\zeta - z)}(1 - \bar{z}\zeta)}{\bar{z}} \log(1 - \bar{z}\zeta). \tag{41}$$

We write $w(z)$ as

$$w(z) = k(|z|^2 - 1) + u_2(z) + V(z) + I(z), \tag{42}$$

where

$$u_2(z) = \frac{1}{2\pi i} \int_{\partial \mathbf{D}} g_1(z, \zeta) h_0(\zeta) \frac{d\zeta}{\zeta}, \tag{43}$$

$$V(z) = \frac{1}{4\pi i} \int_{\partial \mathbf{D}} G_{13}(z, \zeta) h_2(\zeta) \frac{d\zeta}{\zeta}, \tag{44}$$

$$I(z) = -\frac{1}{\pi} \iint_{\mathbf{D}} G_{13}(z, \zeta) f(\zeta) d\xi d\eta. \tag{45}$$

We notice here that $u_2(z)$ is similar to $u_3(z)$ (see (37)). The other two integrals above, namely $V(z)$ and $I(z)$, are evaluated as follows. We write $V(z) = V^{(1)}(z) + V^{(2)}(z) + V^{(3)}(z) + V^{(4)}(z)$ where

$$V^{(1)}(z) = -\frac{1}{4\pi i} \int_{\partial \mathbf{D}} |\zeta - z|^2 \log |\zeta - z|^2 h_2(\zeta) \frac{d\zeta}{\zeta},$$

$$V^{(2)}(z) = -\frac{(1 - |z|^2)}{4\pi i} \int_{\partial \mathbf{D}} \left(4 + \frac{(1 - z\bar{\zeta})}{z\bar{\zeta}} \log(1 - z\bar{\zeta}) + \frac{(1 - \bar{z}\zeta)}{\bar{z}\zeta} \log(1 - \bar{z}\zeta) \right) h_2(\zeta) \frac{d\zeta}{\zeta},$$

$$V^{(3)}(z) = -\frac{1}{4\pi i} \int_{\partial \mathbf{D}} \frac{(\zeta - z)(1 - z\bar{\zeta})}{z} \log(1 - z\bar{\zeta}) h_2(\zeta) \frac{d\zeta}{\zeta},$$

$$V^{(4)}(z) = -\frac{1}{4\pi i} \int_{\partial \mathbf{D}} \frac{\overline{(\zeta - z)(1 - z\bar{\zeta})}}{\bar{z}} \log(1 - \bar{z}\zeta) h_2(\zeta) \frac{d\zeta}{\zeta}.$$

Also we write $I(z) = I_5(z) - I_6'(z) - I_7'(z) + I_8(z) + I_9(z) + I_{10}(z)$ where $I_5(z)$ is given in (11) and where

$$I_6'(z) = \frac{(1 - |z|^2)}{\pi z} \int_{\mathbf{D}} \frac{(1 - z\bar{\zeta}) \log(1 - z\bar{\zeta})}{\bar{\zeta}} f(\zeta) d\xi d\eta,$$

$$I_7'(z) = \frac{(1 - |z|^2)}{\pi \bar{z}} \int_{\mathbf{D}} \frac{(1 - \zeta\bar{z})}{\zeta} \log(1 - \zeta\bar{z}) f(\zeta) d\xi d\eta,$$

$$I_8(z) = \frac{4}{\pi} (1 - |z|^2) \iint_{\mathbf{D}} f(\zeta) d\xi d\eta,$$

$$I_9(z) = \frac{1}{\pi} \iint_{\mathbf{D}} \frac{(\zeta - z)(1 - z\bar{\zeta})}{z} \log(1 - z\bar{\zeta}) f(\zeta) d\xi d\eta,$$

$$I_{10}(z) = \frac{1}{\pi} \iint_{\mathbf{D}} \frac{\overline{(\zeta - z)(1 - \bar{z}\zeta)}}{\bar{z}} \log(1 - \bar{z}\zeta) f(\zeta) d\xi d\eta.$$

We now consider the following theorem for the Fourier coefficients of the solution to the (D4) biharmonic problem but the details for the coefficients are provided in the Appendix.

Theorem 8. *If $w(r, \alpha)$ is the solution of the* (D4) *biharmonic problem mentioned in Thm. 7, and* $z = re^{i\alpha}$, $f(re^{i\alpha}) = \sum_{n=-\infty}^{\infty} f_n(r) e^{in\alpha}, h_0(e^{i\alpha}) = \sum_{n=-\infty}^{\infty} a_n e^{in\alpha}$, *and* $h_2(e^{i\alpha}) = \sum_{n=-\infty}^{\infty} c_n e^{in\alpha}$, *then the Fourier coefficients $\omega_n(r)$ of $\omega(r, \alpha)$ can be written as $w_n(r) = u_{2,n}(r) + V_n^{(1)}(r) + V_n^{(2)}(r) + V_n^{(3)}(r) + V_n^{(4)}(r) - I_{5,n}(r) - I_{6,n}(r) - I_{7,n}(r) + I_{8,n}(r) + I_{9,n}(r) + I_{10,n}(r)$, where the Fourier coefficients of the integrals are given in the Appendix.*

Summary: Before we move on to the next section, we summarize some salient features of the above theorems involving the Fourier coefficients of solutions of four types of biharmonic problems

discussed above. In the theorems 2, 4, 6, and 8, expressions for the Fourier coefficients of solutions of the four biharmonic problems are given. They all involve $I_{5,n}(r)$ which is explicitly given in the theorem 2 (see (20) through (23)). As can be seen from these expressions, evaluation of $I_{5,n}(r)$ requires numerical evaluation of one-dimensional integrals. In the next subsection, we develop some recursive relations (see (48) and (52)) for these integrals which are at the heart of the fast algorithms presented in the next section 3. These recursive relations are compactly written using notations which we introduce first in the subsection below before writing down the recursive relations.

2.5 Recursive Relations

As mentioned above, we introduce below some notations purely for the convenience of developing the recursive relations (48), (49), (52) and (53) for the singular integral $I_5(z)$ which will be used in the development of the fast algorithms in section 3. We define the following for $(j, k) = (1, 1)$ and $(2, 3)$,

$$p_{1,n}^{(j)}(r) = -2 \int_0^r f_n(\rho) \left(\frac{\rho}{r}\right)^n \frac{\rho^k}{n} d\rho, \quad \text{if} \quad n > 0$$

$$p_{2,n}^{(j)}(r) = -2 \int_r^1 f_n(\rho) \left(\frac{r}{\rho}\right)^n \frac{\rho^k}{n} d\rho, \quad \text{if} \quad n > 0$$

$$s_{1,n}^{(j)}(r) = 2 \int_0^r f_n(\rho) \left(\frac{r}{\rho}\right)^n \frac{\rho^k}{n} d\rho, \quad \text{if} \quad n < 0$$

$$s_{2,n}^{(j)}(r) = 2 \int_r^1 f_n(\rho) \left(\frac{\rho}{r}\right)^n \frac{\rho^k}{n} d\rho, \quad \text{if} \quad n < 0$$

$$t_{1,0}^{(j)}(r) = 4 \int_0^r f_0(\rho) \left(\frac{\rho}{r}\right)^k d\rho,$$

$$t_{2,0}^{(j)}(r) = 4 \int_r^1 f_0(\rho) \rho^k \log \rho \, d\rho.$$

For $(j, k) = (3, -1)$ when $n > -1$ and for $(j, k) = (4, 1)$ when $n > 1$, we define

$$p_{1,n}^{(j)}(r) = 2 \int_0^r f_n(\rho) \left(\frac{\rho}{r}\right)^{(n-k)} \frac{\rho^2}{(n-k)} d\rho,$$

$$p_{2,n}^{(j)}(r) = 2 \int_r^1 f_n(\rho) \left(\frac{r}{\rho}\right)^{(n-k)} \frac{\rho^2}{(n-k)} d\rho,$$

$$s_{1,n}^{(j)}(r) = -2 \int_0^r f_n(\rho) \left(\frac{r}{\rho}\right)^{(n-k)} \frac{\rho^2}{(n-k)} d\rho,$$

$$s_{2,n}^{(j)}(r) = -2 \int_r^1 f_n(\rho) \left(\frac{\rho}{r}\right)^{(n-k)} \frac{\rho^k}{(n-k)} d\rho,$$

$$t_{1,k}^{(j)}(r) = -4 \int_0^r f_k(\rho) \rho^2 d\rho,$$

$$t_{2,k}^{(j)}(r) = -4 \int_r^1 f_k(\rho) \rho^2 \log \rho \, d\rho.$$

Corollary 1. *It follows from the notations above that* $p_{1,n}^{(j)}(0) = p_{2,n}^{(j)}(1) = s_{1,n}^{(j)}(0) = s_{2,n}^{(j)}(1) = t_{1,n}^{(j)}(0) = t_{2,n}^{(j)}(1) = 0$, *for* $j = 1, 2, 3, 4$, *and for values of* n *given above.*

Corollary 2. *Let* $0 < r_1 < r_2 < \cdots \cdots < r_M = 1$. *For* $r_j > r_i$, $1 \le i, j \le M$ *if*

$$A_{n,1}^{i,j} = 2 \int_{r_i}^{r_j} f_n(\rho) \left(\frac{R_A}{\rho}\right)^n \frac{\rho}{n} d\rho, \qquad B_{n,1}^{i,j} = 2 \int_{r_i}^{r_j} f_n(\rho) \left(\frac{\rho}{R_B}\right)^n \frac{\rho}{n} d\rho, \tag{46}$$

and

$$A_{0,1}^{i,j} = 4 \int_{r_i}^{r_j} f_0(\rho) \left(\frac{\rho}{r_j}\right) d\rho, \qquad B_{0,1}^{i,j} = 4 \int_{r_i}^{r_j} f_0(\rho) \rho \log \rho \, d\rho, \tag{47}$$

where

$$R_A = \begin{cases} r_i, & \text{if } n > 0, \\ r_j, & \text{if } n < 0, \end{cases} \qquad R_B = \begin{cases} r_j, & \text{if } n > 0, \\ r_i, & \text{if } n < 0, \end{cases}$$

11

then for $1 \leq i, j \leq M$ and $r_l < r_i < r_j$ we have

$$
\begin{cases}
p_{1,n}^{(1)}(r_i) = & \left(\frac{r_l}{r_i}\right)^n p_{1,n}^{(1)}(r_l) - B_{n,1}^{l,i}, & \text{if } n > 0, \\
p_{2,n}^{(1)}(r_i) = & \left(\frac{r_i}{r_j}\right)^n p_{2,n}^{(1)}(r_j) - A_{n,1}^{i,j}, & \text{if } n > 0, \\
s_{1,n}^{(1)}(r_i) = & \left(\frac{r_i}{r_l}\right)^n s_{1,n}^{(1)}(r_l) + A_{n,1}^{l,i}, & \text{if } n < 0, \\
s_{2,n}^{(1)}(r_i) = & \left(\frac{r_j}{r_i}\right)^n s_{2,n}^{(1)}(r_j) + B_{n,1}^{l,j}, & \text{if } n < 0, \\
t_{1,0}^{(1)}(r_i) = & \left(\frac{r_l}{r_i}\right) t_{1,0}^{(1)}(r_l) + A_{0,1}^{l,i}, & \\
t_{2,0}^{(1)}(r_i) = & t_{2,0}^{(1)}(r_j) + B_{0,1}^{i,j},
\end{cases}
\tag{48}
$$

and

$$
I_{5,n}^{(1)}(r_i) = \begin{cases}
r_i^2 \left(r_i \log r_i t_{1,n}^{(1)}(r_l) + t_{2,n}^{(1)}(r_i) \right), & \text{if } n = 0, \\
r_i^2 \left(p_{1,n}^{(1)}(r_i) + p_{2,n}^{(1)}(r_i) \right), & \text{if } n > 0, \\
r_i^2 \left(s_{1,n}^{(1)}(r_i) + s_{2,n}^{(1)}(r_i) \right), & \text{if } n < 0,
\end{cases}
\tag{49}
$$

In a similar fashion with definitions of $A_{n,2}^{i,j}, B_{n,2}^{i,j}$ for $1 \leq i, j \leq M$ we build the recursive relations for $I_{5,n}^{(2)}(r)$.

Corollary 3. *Let $0 < r_1 < r_2 < \cdots\cdots < r_M = 1$ and for $r_j > r_i$, $1 \leq i, j \leq M$ if*

$$
A_{n,3}^{i,j} = 2 \int_{r_i}^{r_j} f_n(\rho) \left(\frac{R}{\rho}\right)^{(n+1)} \frac{\rho^2}{(n+1)} \, d\rho, \qquad
B_{n,3}^{i,j} = 2 \int_{r_i}^{r_j} f_n(\rho) \left(\frac{\rho}{R}\right)^{(n+1)} \frac{\rho^3}{(n+1)} \, d\rho, \tag{50}
$$

and

$$
A_{-1,3}^{i,j} = 4 \int_{r_i}^{r_j} f_{-1}(\rho) \rho^2 \, d\rho, \qquad
B_{-1,3}^{i,j} = 4 \int_{r_i}^{r_j} f_{-1}(\rho) \rho^2 \log \rho \, d\rho. \tag{51}
$$

where

$$
R_A = \begin{cases} r_i, & \text{if } n > -1, \\ r_j, & \text{if } n < -1, \end{cases} \qquad
R_B = \begin{cases} r_j, & \text{if } n > -1, \\ r_i, & \text{if } n < -1, \end{cases}
$$

then for $l = 1 \cdots\cdots M$ and $r_l < r_i < r_j$ we have

$$
\begin{cases}
p_{1,n}^{(3)}(r_i) = & \left(\frac{r_l}{r_i}\right)^{(n+1)} p_{1,n}^{(3)}(r_l) + B_{n,3}^{l,i}, & \text{if } n > -1, \\
p_{2,n}^{(3)}(r_i) = & \left(\frac{r_i}{r_j}\right)^{(n+1)} p_{2,n}^{(3)}(r_j) + A_{n,3}^{i,j}, & \text{if } n > -1, \\
s_{1,n}^{(3)}(r_i) = & \left(\frac{r_i}{r_l}\right)^{(n+1)} s_{1,n}^{(3)}(r_l) - A_{n,3}^{l,i}, & \text{if } n < -1, \\
s_{2,n}^{(3)}(r_i) = & \left(\frac{r_j}{r_i}\right)^{(n+1)} s_{2,n}^{(3)}(r_j) - B_{n,3}^{l,j}, & \text{if } n < -1, \\
t_{1,-1}^{(3)}(r_i) = & t_{1,-1}^{(3)}(r_l) - A_{-1,3}^{l,i}, & \\
t_{2,-1}^{(3)}(r_i) = & t_{2,-1}^{(3)}(r_j) - B_{-1,3}^{i,j},
\end{cases}
\tag{52}
$$

and

$$
I_{5,n}^{(3)}(r_i) = \begin{cases}
r_i \log r_i t_{1,n}^{(3)}(r_i) + r_i t_{2,n}^{(3)}(r_i), & \text{if } n = -1, \\
r_i \left(p_{1,n}^{(3)}(r_i) + p_{2,n}^{(3)}(r_i) \right), & \text{if } n > -1, \\
r_i \left(s_{1,n}^{(3)}(r_i) + s_{2,n}^{(3)}(r_i) \right), & \text{if } n < -1,
\end{cases}
\tag{53}
$$

Applying similar idea and with similar definitions of $A_{n,4}^{i,j}, B_{n,4}^{i,j}$ for $1 \leq i, j \leq M$, we build the recursive relations for $I_{5,n}^{(4)}(r)$. In the case when the inhomogeneous term f and the boundary conditions are real, the relation $f_n = \overline{f_{-n}}$ can be exploited to avoid some of the recursive relations. These recursive relations can be further simplified in this case. For details in the context of such algorithms for problems involving Poisson's equation, see Borges and Daripa [10]. Such simplified recursive relations have been made use of in solving fluid flow problems discussed in Sec. 5.

2.6 Quadrature Method

We discuss here the quadrature methods employed to compute $A^{i,j}_{n,k}$ and $B^{i,j}_{n,k}$. We use Trapezoidal rule and Euler-Maclaurin expansion to compute the integrals. Here we provide some theorems from Sidi and Israeli [34] for the Euler-Maclaurin expansion that we have used for computing the integrals. Let $x_l = a + lh$, $l = 0, 1, ..M$, $h = \frac{b-a}{M}$ and M a positive integer. We state the following theorems.

Theorem 9. *If a function $f(x)$ is $2n$ times differentiable on $[a,b]$ then*

$$\int_a^b f(x)dx = h\sum_{i=0}^{\dot{m}} f(x_i) + \sum_{\nu=1}^{n-1} \frac{B_{2\nu}}{2\nu}[f^{(2\nu-1)}(a) - f^{(2\nu-1)}(b)]h^{2\nu} + R_{2n}[f;(a,b)]$$

where

$$R_{2n}[f;(a,b)] = h^{2n} \int_a^b \frac{\bar{B}_{2n}[(x-a)/h] - B_{2n}}{2n} f^{(2n)}(x)dx.$$

B_ν are the Bernoulli numbers and $\bar{B}_\nu(x)$ are periodic Bernoullian function of order ν and $\sum_{i=0}^{\dot{m}} f(x_i)$ is the summation with the first and the last terms multiplied with $\frac{1}{2}$.

Theorem 10. *If a function $f(x)$ is $2n$ times differentiable on $[a,b]$ and $F(x) = (x-a)^s f(x), s > -1$ then*

$$\int_a^b F(x)dx = h\sum_{i=1}^{\dot{m}} F(x_i) - \sum_{\nu=1}^{n-1} \frac{B_{2\nu}}{(2\nu)!}[F^{(2\nu-1)}(b)h^{2\nu} - \sum_{\nu=0}^{2n-1} \frac{\zeta(-s-\nu)}{\nu!} f^{(\nu)(a)}h^{\nu+s+1} + \rho_{2n}$$

where $\zeta(t)$ is the Riemann zeta function for $Re(t) > 1$ and $\rho_{2n} = \mathcal{O}(h^{2n})$ as $h \to 0$.

In our implementation to compute $A^{i,j}_{n,k}$ and $B^{i,j}_{n,k}$, we used $m = 1$ for each $i = 1, 2...M$ and the first order derivative of the integrands of $A^{i,j}_{n,k}$ and $B^{i,j}_{n,k}$ are computed for $\nu = 1$, to incorporate the correction term as given in the theorems. These theorems provide a very high order accuracy for computing $A^{i,j}_{n,k}$ and $B^{i,j}_{n,k}$.

3 Fast Algorithms

Recall where problems (D1), (D2), (D3) and (D4) are introduced in the paper. We now build fast, high order accurate algorithms for solving the biharmonic problems. Below the numerical algorithms are presented only for problems (D1) and (D2). The algorithms for problems (D3) and (D3) are similar and can be easily formulated. For the fast algorithms developed below, the unit disk is discretized into $M \times N$ equidistant points, M in the radial direction and N in the angular direction. Let $0 = r_1 < r_2 < \ldots < r_M = 1$.

3.1 Algorithm for (D1) biharmonic problem

Now we consider the algorithm for the (D1) biharmonic problem. The algorithm is similar for the (D3) biharmonic problem.

Initialization: Choose M and N. Define $K = \frac{N}{2}$.

Inputs: $M, N, h_0(e^{\frac{2\pi ik}{N}}), h_1(e^{\frac{2\pi ik}{N}}), f(r_l e^{\frac{2\pi ik}{N}})$, for $l = 1, \cdots, M$, for $k = 1, \cdots, N$.

Step 1. Compute the Fourier coefficients a_n, b_n, f_n using FFT for $n = (-K+1), \cdots, K$.

Step 2. Compute $u_{2,n}(r_l)$, $v_{2,n}(r_l)$, $r_{2,n}(r_l)$, $I_{3,n}(r_l)$, $I^{(k)}_{4,n}(r_l)$ to obtain $I_3(z), I_4(z), u_2(z), v_2(z), r_2(z)$ using (12), (13), (14), (15), (16), (17), (18), (19) respectively for $n = (-K+1), \cdots, K$, for $l = 1, \cdots M$, and for $k = 1, \cdots, 4$

Step 3. Compute $A^{i,i+1}_{n,k}, B^{i,i+1}_{n,k}$ for $i = 1 \cdots, (M-1)$, for $n = (-K+1), \cdots, K$, and for $k = 1, \cdots, 4$ using (46), (47), (50), (51) in Corollaries 2 and 3.

Step 4. Compute the recursive relations $p^{(j)}_{1,n}(r_l)$, $p^{(j)}_{2,n}(r_l)$, $t^{(j)}_{1,n}(r_l)$, $t^{(j)}_{2,n}(r_l)$ for $n = 0, \cdots, K$

and $s_{1,n}^{(j)}(r_l)$, $s_{2,n}^{(j)}(r_l)$ for $n = (-K + 1), \cdots, -1$, for $j = 1, \cdots, 4$ and for $l = 1, \cdots, M$ using Corollaries 2 and 3 as shown in the following pseudocodes.

Algorithm: Computation of $p_{1,n}^{(j)}(r_l)\ for$ j=1,2, $p_{1,n}^{(3)}(r_l)$, $p_{1,n}^{(4)}(r_l)$ using recursive relations.

Set $p_{1,n}^{(j)}(r_1 = 0) = 0$;
for $n = 1, \cdots, K$ **do**

 for $l = 2, \cdots, M$ **do**

  $p_{1,n}^{(j)}(r_l) = \left(\dfrac{r_{l-1}}{r_l}\right)^n p_{1,n}^{(j)}(r_{l-1}) - B_{n,j}^{l-1,l}$;

 end

end

Set $p_{1,n}^{(3)}(r_1 = 0) = 0$;
for $n = 0, \cdots, K$ **do**

 for $l = 2, \cdots, M$ **do**

  $p_{1,n}^{(3)}(r_l) = \left(\dfrac{r_{l-1}}{r_l}\right)^{(n+1)} p_{1,n}^{(3)}(r_{l-1}) + B_{n,3}^{l-1,l}$;

 end

end

Set $p_{1,n}^{(4)}(r_1 = 0) = 0$;
for $n = 2, \cdots, K$ **do**

 for $l = 2, \cdots, M$ **do**

  $p_{1,n}^{(4)}(r_l) = \left(\dfrac{r_{l-1}}{r_l}\right)^{(n-1)} p_{1,n}^{(4)}(r_{l-1}) + B_{n,4}^{l-1,l}$;

 end

end

Algorithm: Computation of $p_{2,n}^{(j)}(r_l)\ for$ j=1,2, $p_{2,n}^{(3)}(r_l)$, $p_{2,n}^{(4)}(r_l)$ using recursive relations.

Set $p_{2,n}^{(j)}(r_M = 1) = 0$;
for $n = 1, \cdots, K$ **do**

 for $l = (M - 1), \cdots, 1$ **do**

  $p_{2,n}^{(j)}(r_l) = \left(\dfrac{r_l}{r_{l+1}}\right)^n p_{2,n}^{(j)}(r_{l+1}) - A_{n,j}^{l,l+1}$;

 end

end

Set $p_{2,n}^{(3)}(r_M = 1) = 0$;
for $n = 0, \cdots, K$ **do**

 for $l = (M - 1), \cdots, 1$ **do**

  $p_{2,n}^{(3)}(r_l) = \left(\dfrac{r_l}{r_{l+1}}\right)^{(n+1)} p_{2,n}^{(3)}(r_{l+1}) + A_{n,3}^{l,l+1}$;

 end

end

Set $p_{2,n}^{(4)}(r_M = 1) = 0$;
for $n = 2, \cdots, K$ **do**

 for $l = (M - 1), \cdots, 1$ **do**

  $p_{2,n}^{(4)}(r_l) = \left(\dfrac{r_l}{r_{l+1}}\right)^{(n-1)} p_{2,n}^{(4)}(r_{l+1}) + A_{n,4}^{l,l+1}$;

 end

end

Step 5. Compute $I_{5,n}(r_l)$, for $n = (-K + 1), \cdots, K$, for $l = 1, \cdots, M$ using Corollaries 2 and 3.

Step 6. Finally compute $\omega(r_l e^{\frac{2\pi i k}{N}}) = \sum\limits_{n=-K+1}^{K} (u_2(r_l) + v_2(r_l) + r_2(r_l) + I_3(r_l) + I_4(r_l) + I_5(r_l))\, e^{\frac{2\pi n i k}{N}}$

14

Algorithm: Computation of $s_{1,n}^{(j)}(r_l)$ *for* j=1,2, $s_{1,n}^{(3)}(r_l)$, $s_{1,n}^{(4)}(r_l)$ using recursive relations.

Set $s_{1,n}^{(j)}(r_1 = 0) = 0$;

for $n = -K, \cdots, -1$ **do**

    for $l = 2, \cdots, M$ **do**

        $s_{1,n}^{(j)}(r_l) = \left(\frac{r_l}{r_{l-1}}\right)^n s_{1,n}^{(j)}(r_{l-1}) + A_{n,j}^{l-1,l}$;

    end

end

Set $s_{1,n}^{(3)}(r_1 = 0) = 0$;

for $n = -K, \cdots, -2$ **do**

    for $l = 2, \cdots, M$ **do**

        $s_{1,n}^{(3)}(r_l) = \left(\frac{r_l}{r_{l-1}}\right)^{(n+1)} s_{1,n}^{(3)}(r_{l-1}) - A_{n,3}^{l-1,l}$;

    end

end

Set $s_{1,n}^{(4)}(r_1 = 0) = 0$;

for $n = -K, \cdots, 0$ **do**

    for $l = 2, \cdots, M$ **do**

        $s_{1,n}^{(4)}(r_l) = \left(\frac{r_l}{r_{l-1}}\right)^{(n-1)} s_{1,n}^{(4)}(r_{l-1}) - A_{n,4}^{l-1,l}$;

    end

end

---

using FFT for $k = 1, \cdots, N$, $l = 1, \cdots, M$.

3.2 Algorithm for (D2) biharmonic problem

Now we consider the algorithm for the (D2) biharmonic problem. The algorithm is similar for the (D4) biharmonic problem.

Initialization: Choose M and N. Define $K = \frac{N}{2}$.

Inputs: M, N, $h_0(e^{\frac{2\pi i k}{N}})$, $h_2(e^{\frac{2\pi i k}{N}})$, $f(r_l e^{\frac{2\pi i k}{N}})$, for $l = 1, \cdots, M$, for $k = 1, \cdots, N$.

Step 1. Compute the Fourier coefficients a_n, c_n, f_n using FFT for $n = (-K + 1), \cdots, K$.

Step 2. Compute $u_{2,n}(r_l)$, $v_{3,n}(r_l)$, $I_{4,n}^{(k)}(r_l)$, $I_{6,n}(r_l)$, $I_{7,n}(r_l)$, to obtain $I_4(z)$, $I_6(z)$, $I_7(z)$ using (12), (35), (16), (17), (18) (19), (33), (34) respectively for $n = (-K+1), \cdots, K$, for $l = 1, \cdots, M$, and for $k = 1, \cdots, 4$.

Step 3. Compute $A_{n,k}^{i,i+1}$, $B_{n,k}^{i,i+1}$ for $i = 1, \cdots (M-1)$, for $n = (-K+1), \cdots, K$, and for $k = 1, \cdots, 4$ using (46), (47), (50), (51) in Corollaries 2 and 3.

Step 4. Compute $p_{1,n}^{(j)}(r_l)$, $p_{2,n}^{(j)}(r_l)$ for $n = 1, \cdots, K$ and $s_{1,n}^{(j)}(r_l)$, $s_{2,n}^{(j)}(r_l)$ for $n = (-K + 1), \cdots, -1$ $t_{1,0}^j(r_l)$, $t_{2,0}^j(r_l)$, for $j = 1, \cdots, 4$ and for $l = 1, \cdots, M$ using Corollaries 2 and 3 with the following recursive relations as in the previous algorithm with (D1) biharmonic problem.

Step 5. Compute $I_{5,n}(r_l)$, for $n = (-K + 1), \cdots, K$ and $l = 1, \cdots, M$ using Corollaries 2 and 3.

Step 6. Finally compute $\omega(r_l e^{\frac{2\pi i k}{N}})$ using FFT for $k = 1, \cdots, N$, $l = 1, \cdots, M$.

3.3 Computational Complexity

The asymptotic operation counts for the (D1) biharmonic problem is discussed in Table 1. It is the same for all other problems. The table shows that the theoretical computational complexity is of the order of $O(\log N)$ per point where N^2 is the total number of degrees of freedom.

3.4 Parallel Algorithms

The FFTRR-based methods offer good parallelization opportunities. The intrinsic parallelism in the sequential fast algorithms given in section 3 can be identified in steps 1 and 6 where two

Algorithm: Computation of $s_{2,n}^{(j)}(r_l) \, for$ j=1,2, $s_{2,n}^{(3)}(r_l)$, $s_{2,n}^{(4)}(r_l)$ using recursive relations.

Set $s_{2,n}^{(j)}(r_M = 1) = 0$;
for $n = -K, \cdots, -1$ **do**
    for $l = (M-1), \cdots, 1$ **do**
        $s_{2,n}^{(j)}(r_l) = \left(\frac{r_{l+1}}{r_l}\right)^n s_{2,n}^{(j)}(r_{l+1}) + B_{n,j}^{l,l+1}$;
    end
end
Set $s_{2,n}^{(3)}(r_M = 1) = 0$;
for $n = -K, \cdots, -2$ **do**
    for $l = (M-1), \cdots, 1$ **do**
        $s_{2,n}^{(3)}(r_l) = \left(\frac{r_{l+1}}{r_l}\right)^{(n+1)} s_{2,n}^{(3)}(r_{l+1}) - B_{n,3}^{l,l+1}$;
    end
end
Set $s_{2,n}^{(4)}(r_M = 1) = 0$;
for $n = -K, \cdots, 0$ **do**
    for $l = (M-1), \cdots, 1$ **do**
        $s_{2,n}^{(4)}(r_l) = \left(\frac{r_{l+1}}{r_l}\right)^{(n-1)} s_{2,n}^{(4)}(r_{l+1}) - B_{n,4}^{l,l+1}$;
    end
end

---

groups of Fourier transforms are evaluated independently for each fixed radius. Consequently, their computations can be performed in parallel. Recursive relations also offer efficient implementation of the algorithms by redefining the inherently sequential recurrences present in the sequential algorithms presented above. These and related communication issues between processors have been explained in considerable detail through the formulation of FFTRR-based fast parallel algorithms for the evaluation of singular integrals (see Borges and Daripa [9]) and for the solution of Dirichlet and Neumann problems for Poisson's equation (see Borges and Daripa [10]). Parallel versions of the sequential fast algorithms given in section 3 can be developed using these same principles. Development of such parallel fast algorithms for the biharmonic problems considered in this paper falls outside the scope of this paper and will be taken up in the future.

4   Numerical Results

This section consists of two parts: (i) validation of the algorithms and comparing the accuracy of the method with that of the method based on the "decomposition" method (see [17]); and (ii) application of these to solving low to moderate Reynolds number steady fluid flow problems within a disk. Since the algorithm is based on exact analysis, the error in the numerical computation arises from the evaluation of the one dimensional integrals in the algorithm and the truncation of the Fourier series. The integrands $\rho \log \rho$ and $\rho^2 \log \rho$ in the integrals (47) and (51) respectively varies rapidly near the origin where some care is necessary in accurate evaluation of these integrals. In our implementation, we have found that replacing $\log \rho$ by $\log (\rho + \epsilon)$ with $\epsilon = O(0.01)$ when $r_i = 0$ in these integrals (see (47) and (51)) improves the overall accuracy of the solutions. In the future we will explore in detail on even more accurate evaluation of these integrals which will perhaps help obtain very high order accurate solutions.

Numerical implementations of the algorithms were done in MATLAB and computations were performed using double precision arithmetic. The algorithms were first tested on several examples to validate the algorithms and the code. For each type of biharmonic problems ((D1) through (D4) as described in section 2), the source term and boundary data were generated from the solution of the problem which was chosen a priori. We show computational results using the following examples (identified by the chosen solutions) to highlight some of the accuracy issues we noticed

Algorithm: Computation of $t_{1,0}^{(j)}(r_l)$ *for* j=1,2, $t_{1,-1}^{(3)}(r_l)$, $t_{1,1}^{(4)}(r_l)$ using recursive relations.

Set $t_{1,0}^{(j)}(r_1 = 0) = 0$;
for $l = 2, \cdots, M$ **do**
$\quad \Big|\quad t_{1,0}^{(j)}(r_l) = \left(\frac{r_{l-1}}{r_l}\right) t_{1,0}^{(j)}(r_{l-1}) + A_{0,j}^{l-1,l}$;
end
Set $t_{1,-1}^{(3)}(r_1 = 0) = 0$;
for $l = 2, \cdots, M$ **do**
$\quad \Big|\quad t_{1,-1}^{(3)}(r_l) = t_{1,-1}^{(3)}(r_{l-1}) - A_{-1,3}^{l-1,l}$;
end
Set $t_{1,1}^{(4)}(r_1 = 0) = 0$;
for $l = 2, \cdots, M$ **do**
$\quad \Big|\quad t_{1,1}^{(4)}(r_l) = t_{1,-1}^{(4)}(r_{l-1}) - A_{1,4}^{l-1,l}$;
end

Algorithm: Computation of $t_{2,0}^{(j)}(r_l)$ *for* j=1,2, $t_{2,-1}^{(3)}(r_l)$, $t_{2,1}^{(4)}(r_l)$ using recursive relations.

Set $t_{2,0}^{(j)}(r_M = 0) = 0$;
for $l = (M-1), \cdots, 1$ **do**
$\quad \Big|\quad t_{2,0}^{(j)}(r_l) = t_{2,0}^{(j)}(r_{l+1}) + B_{0,j}^{l,l+1}$;
end
Set $t_{2,-1}^{(3)}(r_M = 1) = 0$;
for $l = (M-1), \cdots, 1$ **do**
$\quad \Big|\quad t_{2,-1}^{(3)}(r_l) = t_{2,-1}^{(3)}(r_{l+1}) - B_{-1,3}^{l,l+1}$;
end
Set $t_{2,1}^{(4)}(r_M = 1) = 0$;
for $l = (M-1), \cdots, 1$ **do**
$\quad \Big|\quad t_{2,1}^{(4)}(r_l) = t_{2,1}^{(4)}(r_{l+1}) - B_{1,4}^{l,l+1}$;
end

---

for the algorithms with these examples. We computationally evaluate the accuracy and complexity of these algorithms below using the following examples (identified by the chosen solutions).

1. $\omega = z^2 \bar{z}^4$.

2. $\omega = i z^3 \bar{z}^4$.

3. $\omega = z^{\frac{3}{2}} \bar{z}^{\frac{5}{2}} + i z^{\frac{5}{2}} \bar{z}^{\frac{9}{2}}$.

We show and discuss the numerical solutions of the (D2) problem for the first example, (D1) and (D3) problems for the second example and (D4) problem for the third example. Tables 2, 3, 4 and 5 show relative errors in the numerical solutions for these problems obtained with the algorithms of the **direct** method presented in this paper. These tables also compare these relative errors with the same obtained with the "decomposition" method presented in Ghosh and Daripa [17]. These tables show that the **direct** method gives fourth order or better accuracy for one case and second order or better accuracy for the other cases. In contrast, the "decomposition" method gives approximate fourth order accuracy for all these cases. The second order accuracy observed in Tables 2 through 4 is due to lower accuracy in the numerical evaluation of the singular integrals involving logarithm for Fourier coefficients with index $n = 0, -1, 1$ (see (46), (51)). The order of accuracy perhaps can be improved with better quadrature methods such as in [22] for numerical evaluation of these weakly singular integrals. We intend to look into this in the future.

Table 1: The complexity at each step for the (D1) biharmonic problem.

Step	Operation Count
1	The M discrete Fourier transforms of N data sets contribute $\mathcal{O}(\mathcal{MN}\log\mathcal{N})$.
2	Computation of $I_{3,n}$, $I_{4,n}$, $u_{2,n}$, $v_{2,n}$, $r_{2,n}$ contribute $\mathcal{O}(\mathcal{MN})$.
3	Computation of $A_{n,j}^{i,i+1}$ and $B_{n,j}^{i,i+1}$, $i = 1, \cdots (M-1)$, $n = (-K+1), \cdots, K$, $j = 1, \cdots, 4$ contribute $\mathcal{O}(\mathcal{MN})$.
4	Computation of each $p_{1,n}^{(j)}$, $p_{2,n}^{(j)}$, $s_{1,n}^{(j)}$, $s_{2,n}^{(j)}$, $t_{1,0}^{(j)}$, $t_{2,0}^{(j)}$, $j = 1, \cdots, 4$ contribute $\mathcal{O}(\mathcal{MN})$.
5	Computation $I_{5,n}(r_l)$, $l = 1, \cdots, M$, $n = (-K+1), \cdots, K$ contribute $\mathcal{O}(\mathcal{MN})$.
6	Computation of $\omega(r_l e^{\frac{2\pi ik}{N}})$, $k = 1, \cdots N, l = 1 \cdots, M$ by FFT contributes $\mathcal{O}(\mathcal{MN}\log\mathcal{N})$ for $M \times N$ grid points.

Table 2: Relative errors for the (D2) Ex.1 in $||\cdot||_\infty$ using Euler-Maclaurin formula with $N = 8$.

M	Direct Method		Decomposition Method	
	$||\cdot||_\infty$	order	$||\cdot||_\infty$	order
16	6.8×10^{-5}	–	4.7×10^{-5}	–
32	2.8×10^{-6}	4.6	2.5×10^{-6}	4.2
64	1.5×10^{-7}	4.2	1.5×10^{-7}	4.1
128	9.2×10^{-9}	4.1	8.9×10^{-9}	4.1
256	5.6×10^{-10}	4.0	5.5×10^{-10}	4.0
512	3.5×10^{-11}	4.0	3.4×10^{-11}	4.0

Table 6 shows results obtained with these two methods for solving the (D2) homogeneous biharmonic problem (see section 2.2) with $f(z) = 0$, $h_0 = 1$ and $h_2 = 1$. It shows that the **direct** method for homogeneous biharmonic problems give spectrally accurate solutions whereas the "decomposition method" gives only second order accurate solutions. This is due to that fact that the boundary integrals involved in the **direct** method are evaluated with spectral accuracy. However, the domain integrals involved in the "decomposition method" are evaluated using the Euler-Maclaurin formulae which has finite order of accuracy. Recall that this same homogeneous biharmonic problem needs to be solved while solving the (D1) and (D3) inhomogeneous biharmonic problems using the "decomposition method" (see [17]). Therefore the "direct method" is an integral part of the "decomposition method" for some boundary value problems and hence it is an important reason to develop the fast algorithms for the **direct** method which are developed in this paper for the first time.

Next we compare numerical asymptotic complexity with our theoretical complexity $O(N^2 \log N)$ where N^2 is the total number of grid points. Complexity of the algorithms has been evaluated based on CPU time required to solve biharmonic problems (D2) and (D3) with different values of N using the Euler-Maclaurin integration scheme. The number of grid points in the radial and azimuthal directions has been taken to be same, N. From this, we also compute the constant c hidden in the order estimate by dividing the total computation time by $N^2 \log N$. The CPU time and the estimate of the constant c for these two problems, (D2) and (D3), have been tabulated in Table 7 for several values of N. The CPU time versus $N^2 \log N$ and computed values of c versus N are shown in Fig. 1(a) and Fig. 1(b) respectively. Figure 1(a) shows that the computationally obtained estimate of the complexity agrees with the theoretical one. Figure 1(b) shows that the constant hidden behind the order estimate of the complexity is indeed very small for large N which is another big advantage for these FFTRR based algorithms. Similar results are obtained for (D1) and (D4) problems. Identical plots as in these figures are obtained when the decomposition algorithm [17], instead of the **direct** method of this paper, is used to solve these problems.

Towards this end, it is worth mentioning that CPU time depends on many parameters including

Table 3: Relative error for the (D1) Ex.2 in $||\cdot||_\infty$ using Euler-Maclaurin formula with $N = 32$.

M	Direct Method $||\cdot||_\infty$	order	Decomposition Method $||\cdot||_\infty$	order
16	5.0×10^{-2}	–	1.2×10^{-3}	–
32	1.2×10^{-2}	2.1	1.0×10^{-4}	3.6
64	3.0×10^{-3}	2.0	8.0×10^{-6}	3.7
128	7.4×10^{-4}	2.0	6.4×10^{-7}	3.6
256	1.8×10^{-4}	2.0	5.2×10^{-8}	3.6
512	4.5×10^{-5}	2.0	4.1×10^{-9}	3.7

Table 4: Relative error for the (D3) Ex.2 in $||\cdot||_\infty$ using Euler-Maclaurin formula with $N = 64$.

M	Direct Method $||\cdot||_\infty$	order	Decomposition Method $||\cdot||_\infty$	order
16	4.4×10^{-1}	–	4.3×10^{-3}	–
32	1.1×10^{-1}	2.0	3.8×10^{-4}	3.5
64	2.7×10^{-2}	2.0	2.6×10^{-5}	3.8
128	6.7×10^{-3}	2.0	1.8×10^{-6}	3.8
256	1.7×10^{-3}	2.0	1.3×10^{-7}	3.7
512	4.1×10^{-4}	2.0	8.4×10^{-9}	3.9

the computational speed of the processor used, precision of the arithmetics (such as 8-digit, 16-digit etc.) used, type of programming language (such as Matlab, C, Fortran, python), issues related to the implementation of algorithms, and code optimization tools used to enhance performance. However, the computational complexity of a specific algorithm does not depend on these factors and this is what has been the motivating factor behind our numerical study leading to the Table 7, Fig. 1(a) and Fig. 1(b). The data in the Table 7 were obtained from computations in a MATLAB 7.9.0(R2009b) version in ASUS A55A series without any kind of Matlab code optimization. The CPU time reported in the table can be improved by many fold depending on how the above parameters on which CPU time depends are chosen. Improvement of CPU time by varying these parameters is altogether a separate topic and falls outside the scope of this paper.

(a) Plot of CPU timings versus $N^2 \log N$ where N^2 is the total number of points in the discretization of the domain.

(b) Plot of $T/(N^2 \log N)$ versus N where N^2 is the total number of points in the discretization of the domain.

Figure 1: Plots of the CPU timings and the constant $c = T/(N^2 \log N)$ for the fast algorithms applied to the biharmonic problems (D2) and (D3) problems using the Euler-Maclaurin formula in the **direct** method. Plots for (D2) and (D3) problems in each of the figures Fig. 1(a) and Fig. 1(b) are indistinguishable from each other.

Table 5: Relative error for the (D4) Ex.3 in $||\cdot||_\infty$ using Euler-Maclaurin formula with $N = 32$.

M	Direct Method		Decomposition Method	
	$||\cdot||_\infty$	order	$||\cdot||_\infty$	order
16	7.0×10^{-2}	–	1.8×10^{-4}	–
32	1.7×10^{-2}	2.0	1.5×10^{-5}	3.6
64	4.1×10^{-3}	2.1	1.2×10^{-6}	3.6
128	1.0×10^{-3}	2.0	1.0×10^{-7}	3.6
256	2.5×10^{-4}	2.0	7.8×10^{-9}	3.7
512	6.2×10^{-5}	2.0	5.8×10^{-10}	3.7

Table 6: Relative errors for the homogeneous (D2) problem in $||\cdot||_\infty$ using Euler-Maclaurin rule with $N = 64$.

M	Direct Method	Decomposition Method	
	$||\cdot||_\infty$	$||\cdot||_\infty$	order
16	7.2×10^{-15}	7.2×10^{-3}	–
32	7.2×10^{-15}	1.4×10^{-3}	2.4
64	7.2×10^{-15}	3.2×10^{-4}	2.1
128	7.2×10^{-15}	7.2×10^{-5}	2.4
256	7.2×10^{-15}	1.7×10^{-5}	2.1
512	7.2×10^{-15}	5.7×10^{-6}	1.6

5   Application to Incompressible Fluid Flows

In this section, we apply these fast, **direct** algorithms to solve steady, viscous, incompressible Navier Stokes equation within a circular cylinder as in [28, 23, 19] generated by the tangential motion of part or all of the boundary and the inflow, outflow of the fluids in which fluid is injected over one portion and ejected radially over another portion of the boundary of the disc. These types of problems arise in recirculation of fluids in cavities and in confined ventilation. The governing equations associated with the steady, viscous, incompressible flow are given by

$$(\mathbf{u} \cdot \nabla)\mathbf{u} = -\nabla p + \nabla \cdot (R^{-1}\nabla\mathbf{u}) \tag{54}$$
$$\nabla \cdot \mathbf{u} = 0, \tag{55}$$

where p is the pressure, R is the Reynolds number, and $\mathbf{u}$ is the velocity. In polar coordinates (r, θ), the velocity is given by $u_r = \frac{1}{r}\frac{\partial \psi}{\partial \theta}, u_\theta = -\frac{\partial \psi}{\partial r}$ in terms of stream function ψ. The vorticty $\boldsymbol{\varphi} = \nabla \times \mathbf{u}$ satisfies $\varphi = -\Delta\psi$. Taking the curl of both sides of (54), we obtain

$$\Delta^2\psi = -RJ[\psi, \Delta\psi], \tag{56}$$

Table 7: CPU times and estimates for the constant c using Euler-Maclaurin formula for (D2) and (D3) problems using the **direct** method.

$M = N$	For the biharmonic problem (D2)		For the biharmonic problem (D3)	
	CPU time in sec.	c	CPU time in sec.	c
16	0.41	5.8×10^{-4}	0.41	5.78×10^{-4}
32	0.44	1.24×10^{-4}	0.45	1.27×10^{-4}
64	0.70	4.11×10^{-5}	0.71	4.17×10^{-5}
128	1.53	1.92×10^{-5}	1.52	1.91×10^{-5}
256	4.12	1.13×10^{-5}	4.25	1.17×10^{-5}
512	12.68	7.75×10^{-6}	12.81	7.83×10^{-6}

where $J[\psi, \Delta\psi] = \frac{1}{r}(\partial_r\psi\partial_\theta\Delta\psi - \partial_r\Delta\psi\partial_\theta\psi)$. Since $(\partial_z\partial_{\bar{z}})^2 = \Delta^2/16$, it follows that the boundary value problem associated with the slow viscous flow problem is given by (see also [28, 23])

$$\left.\begin{aligned}
(\partial_z\partial_{\bar{z}})^2\psi &= -\tfrac{R}{16}J[\psi, \psi_{z\bar{z}}], & \text{in} \quad r < 1, \\
\psi &= f_1(\theta), & \text{on} \quad r = 1, \\
\tfrac{\partial\psi}{\partial r} &= f_2(\theta), & \text{on} \quad r = 1,
\end{aligned}\right\} \tag{57}$$

where boundary data $f_1(\theta)$ and $f_2(\theta)$ come from specific problems to be chosen as we will see below. Notice that this problem (57) is our (D3) biharmonic problem of section 2.3 except that the right hand side of the equation $(57)_1$ is not known a priori. Below, we apply our fast algorithm for this problem from section 3 to solve (57) subject to various boundary conditions using an iteration procedure since the inhomogeneous term depends on the solution itself. This iteration procedure based on the existing body of works (see [19], [28]) is briefly outlined below.

The iteration procedure starts with an initial guess $\psi^{(0)}$ obtained from the solution of Stokes flow problem given by $\psi^{(0)}_{z\bar{z}z\bar{z}} = 0$ subject to the same boundary conditions as below, and then at each $(k+1)$th stage we solve

$$\left.\begin{aligned}
\psi^{(k+1)}_{z\bar{z}z\bar{z}} &= -\tfrac{R}{16}J[\psi^{(k)}, \psi^{(k)}_{z\bar{z}}] & \text{in} \quad r < 1, \\
\psi^{k+1} &= f_1(\theta) & \text{on} \quad r = 1, \\
\tfrac{\partial\psi^{(k+1)}}{\partial r} &= f_2(\theta) & \text{on} \quad r = 1,
\end{aligned}\right\} \tag{58}$$

using our fast algorithm to the (D3) inhomogeneous biharmonic problem. The vorticity φ is obtained through $\varphi = -\Delta\psi$. We continue the iteration until the convergence criterion $\frac{||\psi^{k+1}|| - ||\psi^k||}{||\psi^{k+1}||} <$ tol is met. In our computations, the tolerance 'tol' is taken to be 3×10^{-4}. The Jacobian is obtained using the central difference formula on mesh points inside the disk and either backward or forward difference for points on the boundary.

For the specific problems discussed below, the above iteration scheme diverges for $R > 4$. For $R > 4$, we use a relaxation factor as in the Gauss-Seidel SOR method (see [28]). We start with our initial guess as before to obtain $\psi^{(0)}(z)$ and use the fast algorithm for the (D3) problem to solve for the iterate $\psi^{(k+1)}(z)$ by solving the problem (58). For convergence we use two relaxation factors α and β for fields φ and ψ. To update the values of φ and ψ we use

$$\varphi^{(k+1)}_{n,l} = \alpha\varphi^{\star(k+1)}_{n,l} + (1-\alpha)\varphi^{(k)}_{n,l}, \quad \text{and} \quad \psi^{(k+1)}_{n,l} = \beta\psi^{\star(k+1)}_{n,l} + (1-\beta)\psi^{(k)}_{n,l}.$$

The starred quantities denote values obtained at each iterative step. The relaxation factor helps in convergence and suitable choices for α and β are taken to be 0.3 and 0.5 respectively. The convergence is continued until a given tolerance is reached. This iteration is suitable for problems with moderate Reynolds number and is unstable for problems with high Reynolds number. Next we consider several specific examples.
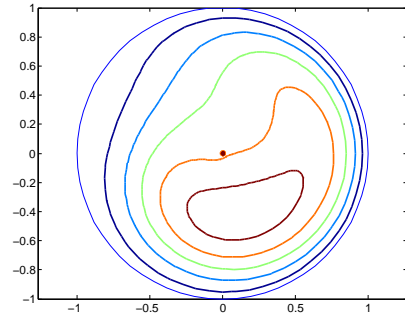
We consider first flows generated by rotation of the circumference as in Mills [28] with $f_1(\theta) = 0$ and $f_2(\theta) = -(1+\cos\theta)/2$. Here Reynolds number $R = Ur/\nu$ where 'r' is the radius of the cylinder, U is the speed of the rotation of the circumference and ν is the kinematic viscosity of the fluid. For studies on similar problems, see [19, 23, 26, 28, 33]. Using the procedure outlined above, the problem (57) with $f_1(\theta) = 0$ and $f_2(\theta) = -(1 + \cos\theta)/2$ is solved numerically using iteration scheme (58) on 64×64 grid points. With tolerance set at 3×10^{-5}, the scheme converged in 30 and 62 iterations respectively for $R = 30$ and $R = 64$. Plots of computed streamlines are shown in Fig. 2. The flow pattern is not symmetric about the x axis and the vortex center is shifted away from the center of the disk. Similar features of the flow have been observed by Imai [23]. Another similar flow problem but now with $f_2(\theta) = -\cos\theta$ was also solved by the same scheme using the same tolerance and the same number of grid points as the above problem. Numbers of iterations taken to converge were 18 and 32 respectively at $R = 16$ and $R = 45$. Plots of streamlines and vorticity patterns are shown respectively in Fig. 3 and Fig. 4. Sharp change in the vorticity is observed with increasing Reynolds number. All of these plots in Fig. 2, Fig. 3 and Fig. 4 are in qualitative agreement with similar plots in Imai [23].

Now we consider the moving wall problem with the boundary condition $\psi(r = 1) = 0$, and the discontinuous boundary condition

$$\left.\frac{\partial\psi}{\partial r}\right|_{r=1} = \begin{cases} -1, & 0 \leq \theta < \pi, \\ 0, & \pi \leq \theta < 2\pi. \end{cases} \tag{59}$$
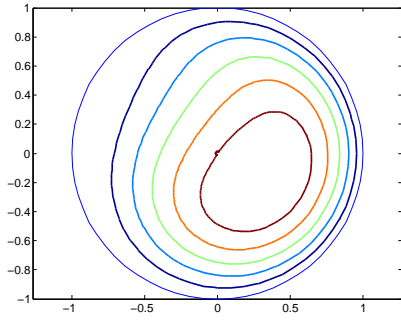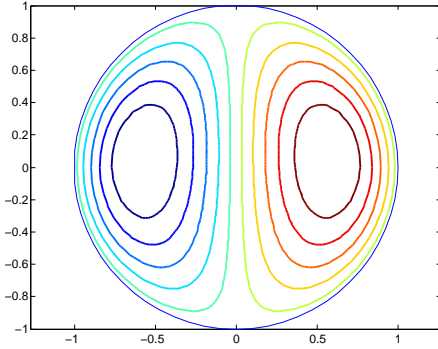
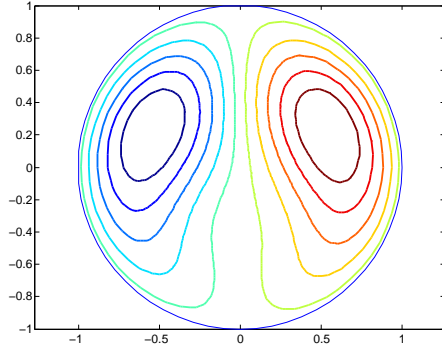(a) streamline patterns for R=30   (b) streamline patterns for R=64

Figure 2: Computed streamline patterns with 64×64 grid points when $f_1(\theta) = 0$ and $f_2(\theta) = -(1 + \cos\theta)/2$
.

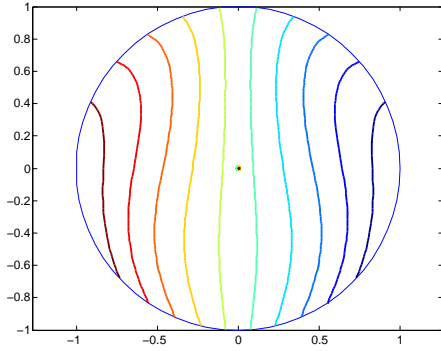(a) streamline patterns for R=16   (b) streamline patterns for R=45

Figure 3: Computed streamline patterns with 64×64 grid points when $f_1(\theta) = 0$ and $f_2(\theta) = -\cos\theta$
.

We computed the flow for several values of R in the interval $0 \leq R \leq 20$ with 128×128 grid points using a tolerance same as in the previous examples. The numbers of iterations were 1 and 27 respectively for $R = 0$ and $R = 10$. The plots of streamline patterns are shown in Fig. 5. We observe a non symmetric flow here with the center of the vortex shifted away from the center of the disk. These results are in qualitative agreement with those by Mills [28] and Mabey [26].
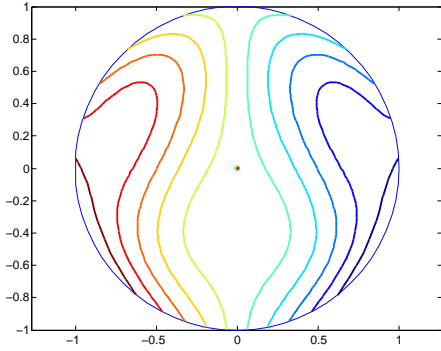
Next we apply our fast algorithm for (D3) biharmonic problem along with the iteration scheme discussed above for computing outflow-inflow problem subject to the following boundary data taken from Mills [28].

$$\left.\frac{\partial\psi}{\partial r}\right|_{r=1} = 0, \quad \& \quad \psi(r=1, \theta) = \begin{cases} 1 + \frac{(\theta-\alpha)}{\epsilon}, & \alpha - \epsilon < \theta < \alpha + \epsilon, \\ 2, & \alpha + \epsilon < \theta < \beta - \epsilon, \\ 1 + \frac{(\beta-\theta)}{\epsilon}, & \beta - \epsilon < \theta < \beta + \epsilon, \\ 0, & \beta + \epsilon < \theta < 2\pi + \alpha - \epsilon. \end{cases} \tag{60}$$

We take $\alpha = 0, \epsilon = \pi/32$ and $\beta = \pi$. The Reynolds number of the flow here is given by $R = U\epsilon/\nu$, where U is the speed and $U\epsilon$ the flow across the arc intercepted by ϵ. Computations were performed with 128×128 grid points using the same tolerance as in the previous examples. Numbers of iterations to converge were 13 and 20 at $R = 0.009$ and $R = 0.02$ respectively. Plots of streamline
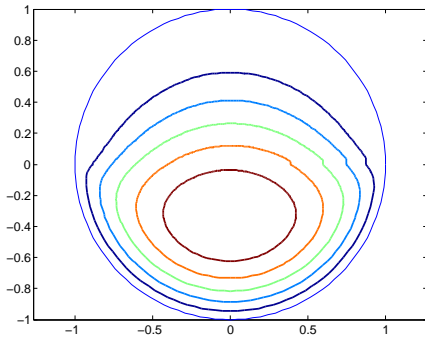
22

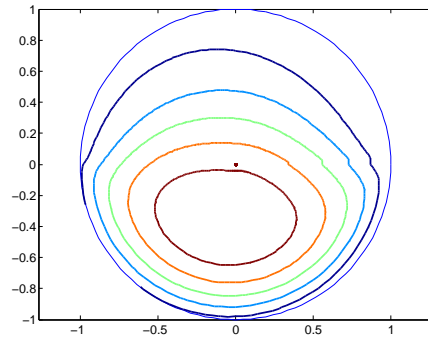(a) vorticity patterns for R=16   (b) vorticity patterns for R=45

Figure 4: Computed vorticity patterns with 64×64 grid points when $f_1(\theta) = 0$ and $f_2(\theta) = -\cos\theta$
.

(a) streamline patterns for R=0   (b) streamline patterns for R=10

Figure 5: Plots of computed streamlines for the moving wall problem with the discontinuous boundary data (59) using 128×128 grid points.

patterns for very low Reynolds number are shown in Fig. 6. This flow has been studied before by Dennis [16]. To compute flows at higher Reynolds numbers, an inexact Newton iteration (see [19]) is required. Such higher Reynolds number flows using our fast algorithm will be computed in the future.

6   Conclusions

In this paper, we have developed FFTRR (FFT and recursive-relation) based accurate and fast algorithms for several biharmonic problems in a unit disc in the complex plane using the "**direct**" method as opposed to the "decomposition" method discussed in Ghosh and Daripa [17]. In the "**direct**" method, solutions of the biharmonic problems are written directly in terms of Green's functions of these problems. The fast algorithms developed here based on the "**direct**" method have been implemented using MATLAB programs. Their performance in terms of accuracy and complexity has been numerically evaluated and presented using several test problems. Computed values of complexity agree with the theoretical computational complexity: $\mathcal{O}(\log \mathcal{N})$ per degree of freedom. These fast algorithms have been applied to solving incompressible slow viscous flow

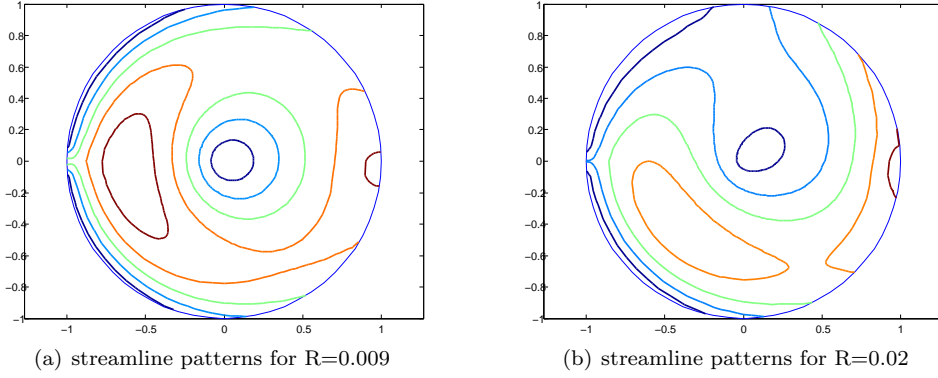(a) streamline patterns for R=0.009   (b) streamline patterns for R=0.02

Figure 6: Plots of computed streamlines for the inflow-outflow problem with the boundary data (60) using 128×128 grid points.

problems at low to moderate Reynolds numbers. The results on these flow problems agree well with the works of others on similar test problems. Application of these algorithms to solving higher Reynolds number flows can be done using inexact Newton iteration since this iteration has been successful in solving higher Reynolds number flows [19]. This is a topic of future research and falls outside the scope of this paper.

Acknowledgments:

Appendix: Proofs of The Theorems

In this section, proofs of the theorems stated in section 2 of this paper are sketched.

Proof 1. (Proof of Thm. 2) *From* (2) *we rewrite* $\omega(z)$ *as*
$\omega(z) = u_2(z) + v_2(z) + r_2(z) + I_3(z) + I_4(z) + I_5(z)$. *We evaluate first,*

$$
\begin{aligned}
I_4(z) &= -\frac{2}{\pi} \iint_{\mathbf{D}} (|\zeta|^2 + |z|^2 - \zeta\bar{z} - \bar{\zeta}z) \log|1 - z\bar{\zeta}| f(\zeta) d\xi d\eta \\
&= I_4^{(1)}(z) + I_4^{(2)}(z) + I_4^{(3)}(z) + I_4^{(4)}(z)
\end{aligned}
$$

where

$$
I_4^{(1)}(z) = -\frac{2r^2}{\pi} \iint_{\mathbf{D}} \log|1 - z\bar{\zeta}| f(\zeta) d\xi d\eta, \qquad I_4^{(2)}(z) = -\frac{2}{\pi} \iint_{\mathbf{D}} \rho^2 \log|1 - z\bar{\zeta}| f(\zeta) d\xi d\eta,
$$

$$
I_4^{(3)}(z) = \frac{2}{\pi} \iint_{\mathbf{D}} \bar{z}\zeta \log|1 - z\bar{\zeta}| f(\zeta) d\xi d\eta, \qquad I_4^{(4)}(z) = \frac{2}{\pi} \iint_{\mathbf{D}} z\bar{\zeta} \log|1 - z\bar{\zeta}| f(\zeta) d\xi d\eta.
$$

Let $I_4^{(1)}(z) = \sum_{n=-\infty}^{\infty} I_{4,n}^{(1)}(r) e^{in\alpha}$ *and* $\alpha - \theta = \tau$. *Then*

$$
\begin{aligned}
I_{4,n}^{(1)}(r) &= -\frac{r^2}{\pi^2} \iint_{\mathbf{D}} f(\zeta) \int_0^{2\pi} \log|1 - z\bar{\zeta}| e^{-in\alpha} d\alpha d\xi d\eta \\
&= 2r^2 \int_0^1 f_n(\rho) G_{4,n}^{(1)}(r,\rho) \rho d\rho,
\end{aligned}
\tag{61}
$$

24

$$\text{where} \qquad G_{4,n}^{(1)}(r,\rho) = -\frac{1}{\pi}\int_0^{2\pi}\log|1 - z\bar{\zeta}|e^{-in\tau}d\tau = \begin{cases} \frac{(r\rho)^{|n|}}{|n|}, & \text{if } n \neq 0 \\ 0. & \text{if } n = 0. \end{cases} \qquad (62)$$

Substituting (62) in (61) we recover the Fourier coefficients of $I_4^{(1)}(z)$. Pursuing similar idea we obtain the Fourier coefficients of $I_4^{(2)}(z), I_4^{(3)}(z), I_4^{(4)}(z)$. Now we evaluate $I_5(z)$ given by (11).

$$I_5(z) = \frac{2r^2}{\pi}\iint\limits_{\mathbf{D}}\log|\zeta - z|f(\zeta)d\xi d\eta + \frac{2}{\pi}\iint\limits_{\mathbf{D}}|\zeta|^2\log|\zeta - z|f(\zeta)d\xi d\eta$$

$$- \frac{2}{\pi}\iint\limits_{\mathbf{D}}\bar{z}\zeta\log|\zeta - z|f(\zeta)d\xi d\eta - \frac{2}{\pi}\iint\limits_{\mathbf{D}}z\bar{\zeta}\log|\zeta - z|f(\zeta)d\xi d\eta \qquad (63)$$

$$= I_5^{(1)}(z) + I_5^{(2)}(z) + I_5^{(3)}(z) + I_5^{(4)}(z). \qquad (64)$$

Notice the singular integral associated with $I_5^{(1)}(z)$ are similar (see [17]) and we compute $I_5^{(3)}(z)$. Let $I_5^{(3)}(z) = \displaystyle\sum_{n=-\infty}^{\infty} I_{5,n}^{(3)}(r)e^{in\alpha}$ where $I_{5,n}^{(3)}(r)$ is similarly given by

$$I_{5,n}^{(3)}(r) = \iint\limits_{\Omega_0^r}\bar{z}\zeta f(\zeta)Q_n^1(r,\zeta)d\xi d\eta + \iint\limits_{\Omega_r^1}\bar{z}\zeta f(\zeta)Q_n^1(r,\zeta)d\xi d\eta, \qquad (65)$$

where $Q_n^1(r,\zeta) = \frac{1}{\pi^2}\int_0^{2\pi}e^{-in\alpha}\bar{z}\log|\zeta - z|d\alpha$. For $r > \rho$, we have

$$Q_n^1(r,\zeta) = \frac{1}{\pi^2}\int_0^{2\pi}e^{-in\alpha}re^{-i\alpha}\left(\log r - \sum_{m\neq 0}\left(\frac{\rho}{r}\right)^{|m|}\frac{1}{2|m|}e^{im\tau}\right)d\alpha$$

$$= \frac{r}{\pi^2}\int_0^{2\pi}e^{-i(n+1)\alpha}\log r\,d\alpha - \frac{r}{\pi^2}\sum_{m\neq 0}\left(\frac{\rho}{r}\right)^{|m|}\frac{1}{2|m|}e^{-im\theta}\int_0^{2\pi}e^{i(m-n-1)\alpha}d\alpha$$

$$= \begin{cases} \frac{r}{\pi|n+1|}\left(\frac{\rho}{r}\right)^{|n+1|}e^{-i(n+1)\theta} & \text{if } n \neq -1, \\ \frac{-2}{\pi}r\log r & \text{if } n = -1. \end{cases} \qquad (66)$$

Similarly, we obtain for $r < \rho$,

$$Q_n^1(r,\zeta) = \begin{cases} \frac{r}{\pi|n+1|}\left(\frac{r}{\rho}\right)^{|n+1|}e^{-i(n+1)\theta}, & \text{if } n \neq -1, \\ -\frac{2}{\pi}r\log\rho, & \text{if } n = -1. \end{cases} \qquad (67)$$

Substituting (66), (67) in (65) we have for $n > -1$,

$$I_{5,n}^{(3)}(r) = \iint\limits_{\Omega_0^r}\zeta f(\zeta)Q_n^1(r,\zeta)d\xi d\eta + \iint\limits_{\Omega_r^1}\zeta f(\zeta)Q_n^1(r,\zeta)d\xi d\eta$$

$$= \frac{r}{\pi(n+1)}\int_0^r\int_0^{2\pi}\rho e^{i\theta}f(\rho e^{i\theta})\left(\frac{\rho}{r}\right)^{(n+1)}e^{-i(n+1)\theta}\rho\,d\theta d\rho$$

$$+ \frac{r}{\pi(n+1)}\int_r^1\int_0^{2\pi}\rho e^{i\theta}f(\rho e^{i\theta})\left(\frac{r}{\rho}\right)^{(n+1)}e^{-i(n+1)\theta}\rho\,d\theta d\rho$$

$$= \frac{r}{\pi(n+1)}\int_0^r\left(\frac{\rho}{r}\right)^{(n+1)}\rho^2\sum_{m=-\infty}^{\infty}f_m(\rho)\int_0^{2\pi}e^{i(m-n)\theta}d\theta d\rho$$

$$+ \frac{r}{\pi(n+1)}\int_r^1\left(\frac{r}{\rho}\right)^{(n+1)}\rho^2\sum_{m=-\infty}^{\infty}f_m(\rho)\int_0^{2\pi}e^{i(m-n)\theta}d\theta d\rho$$

$$= 2r\int_0^r\left(\frac{\rho}{r}\right)^{n+1}\frac{\rho^2}{(n+1)}f_n(\rho)d\rho + 2r\int_r^1\left(\frac{r}{\rho}\right)^{(n+1)}\frac{\rho^2}{(n+1)}f_n(\rho)d\rho. \qquad (68)$$

Similarly, we evaluate for $n < -1$ and $n = -1$ and obtain (22). We evaluate the Fourier Coefficients of the rest in a similar manner. Now let $I_3(z) = \sum\limits_{n=-\infty}^{\infty} I_{3,n}(r)e^{in\alpha}$. Then

$$
\begin{aligned}
I_{3,n}(r) &= \frac{(1-r^2)}{\pi} \int_0^1 (1-\rho^2) \sum_{m=-\infty}^{\infty} f_m(\rho) \int_0^{2\pi} e^{im\theta} \rho\, d\theta\, d\rho, \\
&= 2(1-r^2) \int_0^1 \rho(1-\rho^2) f_0(\rho) d\rho, \\
&= \begin{cases} 2(1-r^2)\int_0^1 \rho(1-\rho^2) f_n(\rho) d\rho, & \text{if } n = 0, \\ 0, & \text{if } n \neq 0. \end{cases}
\end{aligned}
\tag{69}
$$

Thus we recover (15). Now for the boundary integrals $u_2(z)$, $v_2(z)$ and $r_2(z)$ the idea is similar and hence we skip the details.

Proof 2. (Proof of Thm. 4) *We first evaluate the Fourier coefficients $I_{6,n}(r)$ of $I_6(z)$.*

$$
I_{6,n}(r) = \frac{1}{2\pi^2} \iint_{\mathbf{D}} f(\zeta) P_n(r,\zeta) d\xi d\eta,
\tag{70}
$$

where

$$
\begin{aligned}
P_n(r,\zeta) &= (r^2-1)(1-|\zeta|^2) \int_0^{2\pi} e^{-in\alpha} \frac{\log(1-z\bar\zeta)}{z\bar\zeta} d\alpha \\
&= (1-r^2)(1-|\zeta|^2) \sum_{m=1}^{\infty} \frac{(r\bar\zeta)^{(m-1)}}{m} \int_0^{2\pi} e^{-i(m-n-1)\alpha} d\alpha \\
&= \begin{cases} 2\pi \frac{(1-r^2)(1-|\zeta|^2)(r\bar\zeta)^n}{(n+1)}, & \text{if } n \geq 0, \\ 0, & \text{if } n < 0. \end{cases}
\end{aligned}
\tag{71}
$$

Substituting (71) in (70), the formula (33) for $I_{6,n}(r)$ is recovered. Similarly, we obtain $I_{7,n}(r)$. The boundary integrals in the expression (29) for $v_3(z)$ are similarly evaluated to obtain its Fourier coefficient given by (35). The calculations are straightforward and we skip the details. This concludes the proof of Thm. 4.

As for the proof of Thm. 6, the area integrals $I_3(z)$, $I_4(z)$, $I_5(z)$ are same as before and hence details are skipped. The approach to evaluate the boundary integrals are also similar as before so we omit the proof.

Proof 3. (Proof for Thm. 8) *We evaluate $V(z)$ first. Now,*

$$
\begin{aligned}
V^{(1)}(z) &= -\frac{1}{4\pi i} \int_{\partial \mathbf{D}} |\zeta - z|^2 \log|\zeta - z|^2 h_2(\zeta) \frac{d\zeta}{\zeta} \\
&= \frac{1}{2\pi i} \int_{\partial \mathbf{D}} (1 + r^2 - \bar z \zeta - z\bar\zeta) \left(\sum_{n \neq 0} \frac{|z\bar\zeta|^{|n|}}{2|n|} e^{in\tau} \right) h_2(\zeta) \frac{d\zeta}{\zeta} \\
&= V_1^{(1)}(z) + V_2^{(1)}(z) + V_3^{(1)}(z).
\end{aligned}
$$

Let $h_2(e^{i\theta}) = \sum\limits_{n=-\infty}^{\infty} c_n e^{in\theta}$. The Fourier coefficients of the boundary integrals $V_i^{(1)}(z)$ for $i = 1, 2, 3$ are easy to compute. These are given by

$$
V_{1,n}^{(1)}(r) = \begin{cases} \frac{1+r^2}{2n} r^n c_n, & \text{if } n > 0, \\ -\frac{1+r^2}{2n} r^{-n} c_n, & \text{if } n < 0, \\ 0, & \text{if } n = 0. \end{cases}
\qquad
V_{2,n}^{(1)}(r) = \begin{cases} -\frac{r^{n+2}}{2(n+1)} c_n, & \text{if } n > -1, \\ \frac{r^{-n}}{2(n+1)} c_n, & \text{if } n < -1, \\ 0, & \text{if } n = -1. \end{cases}
$$

$$
V_{3,n}^{(1)}(r) = \begin{cases} -\frac{r^n}{2(n-1)} c_n, & \text{if } n > 1, \\ \frac{r^{2-n}}{2(n-1)} c_n, & \text{if } n < 1, \\ 0, & \text{if } n = 1. \end{cases}
$$

Similarly we evaluate $V_n^{(2)}(r)$, $V_n^{(3)}(r)$, $V_n^{(4)}(r)$ and obtain

$$V_n^{(2)}(r) = \begin{cases} (r^2-1)c_0, & \text{if } n = 0, \\ \frac{(r^2-1)r^{|n|}}{2|n|(1+|n|)}c_n, & \text{if } n \neq 0. \end{cases} \tag{72}$$

$$V_n^{(3)}(r) = \begin{cases} \frac{1}{2}c_0, & \text{if } n = 0, \\ -\frac{3}{4}rc_1, & \text{if } n = 1, \\ \frac{r^n}{2(n+1)}c_n - \frac{r^n}{n}c_n + \frac{r^n}{2(n-1)}c_n, & \text{if } n \geq 2. \\ 0, & \text{if } n < 0. \end{cases} \tag{73}$$

$$V_n^{(4)}(r) = \begin{cases} \frac{1}{2}c_n, & \text{if } n = 0, \\ \frac{3}{4}rc_n, & \text{if } n = -1, \\ \frac{r^{-n}}{2(1-n)}c_n - \frac{r^{-n}}{n}c_n - \frac{r^n}{2(n+1)}c_n, & \text{if } n \leq -2, \\ 0, & \text{if } n > 0. \end{cases} \tag{74}$$

Now we evaluate $I_6'(z), I_7'(z), I_8(z), I_9(z)$ and $I_{10}(z)$. The Fourier coefficients of $I_6'(z), I_7'(z)$ are given by

$$I_{6,n}'(r) = \begin{cases} -2(1-r^2)\int_0^1 f_n(\rho)\rho d\rho, & \text{if } n = 0, \\ \frac{2(1-r^2)}{n(n+1)}\int_0^1 (r\rho)^n f_n(\rho)\rho d\rho, & \text{if } n \geq 1 \\ 0 & \text{otherwise} \end{cases} \tag{75}$$

$$I_{7,n}'(r) = \begin{cases} -2(1-r^2)\int_0^1 f_n(\rho)\rho d\rho, & \text{if } n = 0, \\ \frac{2(1-r^2)}{n(n-1)}\int_0^1 (r\rho)^{-n} f_n(\rho)\rho d\rho, & \text{if } n \leq -1 \\ 0 & \text{otherwise} \end{cases} \tag{76}$$

The Fourier coefficients of $I_8(z)$ are given by

$$I_{8,n}(r) = \frac{(1-r^2)}{2\pi^2}\int_{\mathbf{D}} f(\zeta)\int_0^{2\pi} 4e^{-in\alpha}d\alpha d\xi d\eta$$
$$= \begin{cases} 8(1-r^2)\int_0^1 f_n(\rho)\rho d\rho, & \text{if } n = 0, \\ 0, & \text{if } n \neq 0. \end{cases} \tag{77}$$

We write $I_9(z) = I_9^{(1)}(z) + I_9^{(2)}(z)$ where

$$I_9^{(1)}(z) = \frac{1}{\pi z}\int_D \zeta(1 - z\bar\zeta)\log(1 - z\bar\zeta)f(\zeta)d\xi d\eta, \qquad I_9^{(2)}(z) = -\frac{1}{\pi}\int_D (1 - z\bar\zeta)\log(1 - z\bar\zeta)f(\zeta)d\xi d\eta.$$

Now we evaluate $I_{9,n}^{(1)}(r)$.

$$I_{9,n}^{(1)}(r) = \frac{1}{2\pi^2 z}\int_0^1\int_0^{2\pi} f(\rho,\theta)e^{-in\theta}\int_0^{2\pi} \zeta(1 - z\bar\zeta)\log(1 - z\bar\zeta)e^{-in\tau}d\tau\rho d\theta d\rho$$
$$= \begin{cases} -2\int_0^1 f_0(\rho)\rho^3 d\rho, & \text{if } n = 0, \\ \frac{2r^n}{n(n+1)}\int_0^1 \rho^{n+3}f_n(\rho)d\rho, & \text{if } n \geq 1, \\ 0, & \text{if } n < 0. \end{cases} \tag{78}$$

Similarly we obtain

$$I_{9,n}^{(2)}(r) = \begin{cases} 2r\int_0^1 f_n(\rho)\rho^2 d\rho, & \text{if } n = 1, \\ -\frac{2(r^n)}{n(n-1)}\int_0^1 \rho^{n+1}f_n(\rho)d\rho, & \text{if } n \geq 2, \\ 0, & \text{if } n < 1. \end{cases} \tag{79}$$

We now write $I_{10}(z) = I_{10}^{(1)}(z) + I_{10}^{(2)}(z)$ where

$$I_{10}^{(1)}(z) = \frac{1}{\pi \bar{z}} \int_{\mathbf{D}} \bar{\zeta}(1 - \zeta\bar{z}) \log(1 - \zeta\bar{z}) f(\zeta) d\xi d\eta, \qquad I_{10}^{(2)}(z) = -\frac{1}{\pi} \int_{\mathbf{D}} (1 - \zeta\bar{z}) \log(1 - \zeta\bar{z}) f(\zeta) d\xi d\eta.$$

Their Fourier coefficients are easily evaluated which are given by

$$I_{10,n}^{(1)}(r) = \begin{cases} -2 \int_0^1 f_0(\rho)\rho^3 d\rho, & \text{if } n = 0, \\ 2\frac{r^{-n}}{n(n-1)} \int_0^1 \rho^{3-n} f_n(\rho) d\rho, & \text{if } n \leq -1, \\ 0, & \text{if } n > 0. \end{cases} \tag{80}$$

$$I_{10,n}^{(2)}(r) = \begin{cases} 2r \int_0^1 f_{-1}(\rho)\rho^2 d\rho, & \text{if } n = -1, \\ -2\frac{r^{-n}}{n(n+1)} \int_0^1 \rho^{1-n} f_n(\rho) d\rho, & \text{if } n \leq -2, \\ 0, & \text{if } n > -1. \end{cases} \tag{81}$$

References

[1] Andersson, L-E., Elfving, T., Golub, G.: Solution of biharmonic equations with application to radar imaging. *J. Comput. Appl. Math.* 94(2), 153–180 (1998).

[2] Badea, L., Daripa, P.: A fast algorithm for two-dimensional elliptic problems. *Numer. Algorithms.* 30(3-4), 199–239 (2002).

[3] Begehr, H.: Boundary value problems in complex analysis. II. *Bol. Asoc. Mat. Venez.* 12(2), 217–250 (2005).

[4] Begehr, H.: Dirichlet problems for the biharmonic equation. *Gen. Math.* 13(2), 65–72 (2005).

[5] Begehr, H.: Biharmonic Green functions. *Matematiche (Catania)* 61(2) 395–405 (2006).

[6] Begehr, H.: Six biharmonic Dirichlet problems in complex analysis. In *Function spaces in complex and Clifford analysis, edited by Le Hung Son and Wolfgang Tutschke*, Natl. Univ. Publ. Hanoi, 243-252 (2008).

[7] Ben-Artzi, M., Chorev, I., Croisille, J.P., Fishelov, D.: A compact difference scheme for the biharmonic equation in planar irregular domains. *SIAM J. Numer. Anal.* 47(4), 3087–3108 (2009).

[8] Bjorstad, P.: Fast numerical solution of the biharmonic Dirichlet problem on rectangles. *SIAM. J. Numer. Anal.* 20, 626–668 (1983).

[9] Borges, L., Daripa, P.: A parallel version of a fast algorithm for singular integral transforms. *Numer. Algorithms.* 23(1), 71–96 (2000).

[10] Borges, L., Daripa, P.: A fast parallel algorithm for the Poisson equation on a disk. *J. Comput. Phys.* 169(1), 151–192 (2001).

[11] Braess, D., Peisker, P.: On the numerical solution of the biharmonic equation and the role of squaring matrices for preconditioning. *IMA J. Numer. Anal.* 6(4), 393–404 (1986).

[12] Cheng, X., Han, W., Huang, H.: Some mixed finite element methods for biharmonic equation. *J. Comput. Appl. Math.* 126(1-2), 91–109 (2000).

[13] Daripa, P.: A fast algorithm to solve nonhomogeneous Cauchy-Riemann equations in the complex plane. *SIAM J. Sci. Statist. Comput.* 13(6), 1418–1432 (1992).

[14] Daripa, P.: A fast algorithm to solve the Beltrami equation with applications to quasiconformal mappings. *J. Comput. Phys.* 106(2), 355–365 (1993).

[15] Daripa, P., Mashat, D.: Singular integral transforms and fast numerical algorithms. *Numer. Algorithms.* 18(2), 133–157 (1998).

[16] Dennis, S.C.R.: Numerical methods in fluid dynamics. *In Proc. 4th Int. Conf. on Numerical Methods in Fluid Dyn.* 4(0), 138–143 (1974).

[17] Ghosh, A., Daripa, P.: The FFTRR-based fast decomposition methods for solving complex biharmonic problems and incompressible flows. *IMA J. Numer. Anal.* 36(2), 824-850 (2015).

[18] Greenbaum, A., Greengard, L., Mayo, A.: On the numerical solution of the biharmonic equation in the plane. *Phys. D.* 60(1-4), 216–225 (1992). Experimental mathematics: computational issues in nonlinear science (Los Alamos, NM, 1991).

[19] Greengard, L., Kropinski, M.: An integral equation approach to the incompressible Navier-Stokes equations in two dimensions. *SIAM J. Sci. Comput.* 20(1), 318–336 (1998).

[20] Greengard, L., Kropinski, M., Mayo, A.: Integral equation methods for Stokes flow and isotropic elasticity in the plane. *J. Comput. Phys.* 125(2), 403–414 (1996).

[21] Guazzelli, E., Morris, J.F.: *A physical introduction to suspension dynamics.* Cambridge Texts in Applied Mathematics. Cambridge University Press, Cambridge, (2012).

[22] Kapur, S., Rokhlin, V.: High-order corrected trapezoidal quadrature rules for singular functions. *SIAM J. Numer. Anal.* 34(4), 1331–1356 (1997).

[23] Kuwahara, K., Imai, I.: Steady viscous flow within a circular boundary. *Phys. Fluids.* 12(2), 94–101 (1969).

[24] Love, A.E.H.: *A Treatise on the Mathematical Theory of Elasticity.* Dover Press., 1927, reprinted (1994).

[25] Lurie, S.A., Vasiliev, V.V.: *The biharmonic problem in the theory of elasticity.* Gordon and Breach Publishers, Luxembourg, (1995).

[26] Mabey, D.G.: Fluid dynamics. *J.Roy. Aero.Soc.* 61(2), 181–198 (1957).

[27] Mayo, A.: The rapid evaluation of volume integrals of potential theory on general regions. *J. Comput. Phys.* 100(2), 236–245 (1992).

[28] Mills, R.D.: Computing internal viscous flow problems for the circle by integral methods. *J. Fluid Mech.* 79(3), 609–624 (1977).

[29] Monk, P.: A mixed finite element method for the biharmonic equation. *SIAM J. Numer. Anal.* 24(4), 737–749 (1987).

[30] Muskhelishvili, N.I.: *Some Basic Problems of the Mathematical Theory of Elasticity, 3rd (and revised) ed., English translation.* Springer (1977).

[31] Pandit, S.K.: On the use of compact streamfunction-velocity formulation of steady Navier-Stokes equations on geometries beyond rectangular. *J. Sci. Comput.* 36(2), 219–242 (2008).

[32] Peisker, P.: On the numerical solution of the first biharmonic equation. *RAIRO Modél. Math. Anal. Numér.* 22(4), 655–676 (1988).

[33] Rayleigh, L.: Fluid dynamics. *Phil. Mag.* 5(5), 354–363 (1893).

[34] Sidi, A., Israeli, M.: Quadrature methods for periodic singular and weakly singular Fredholm integral equations. *J. Sci. Comput.* 3(2), 201–231 (1988).

[35] Wang, Z., Wei, X., Gao, X.: Solution of the plane stress problems of strain-hardening materials described by power-law using the complex pseudo-stress function. *Appl. Math. Mech.* 12(5), 481–492 (1991).